© 2010 International Press
Adv. Theor. Math. Phys. **14** (2010) 643–694

Supersymmetry, lattice fermions, independence complexes and cohomology theory

Liza Huijse[1,2] **and Kareljan Schoutens**[1]

[1]Institute for Theoretical Physics, University of Amsterdam,
Science Park 904, 1090 GL Amsterdam, the Netherlands
C.J.M.Schoutens@uva.nl
[2]Department of Physics, Harvard University,
17 Oxford Street, Cambridge MA 02138, USA

Abstract

We analyze the quantum ground state structure of a specific model of itinerant, strongly interacting lattice fermions. The interactions are tuned to make the model supersymmetric. Due to this, quantum ground states are in one-to-one correspondence with cohomology classes of the so-called independence complex of the lattice. Our main result is a complete description of the cohomology, and thereby of the quantum ground states, for a two-dimensional square lattice with periodic boundary conditions. Our work builds on results by Jonsson, who determined the Euler characteristic (Witten index) via a correspondence with rhombus tilings of the plane. We prove a theorem, first conjectured by Fendley, which relates dimensions of the cohomology at grade n to the number of rhombus tilings with n rhombi.

e-print archive: http://lanl.arXiv.org/abs/0903.0784

1 Introduction

The motivation for the work presented in this paper is multi-faceted. On the physics side, the motivation stems from the need to understand the electronic properties of materials where electrons are free to move but subject to strong (repulsive) interactions. Even at the level of relatively simple model Hamiltonians, the behavior of such systems is notoriously difficult to analyze. The model studied in this paper has been chosen such that it enjoys a property called supersymmetry [1]. The benefit of this has turned out to be two-fold. First, the supersymmetry leads to a considerable degree of analytic control, allowing the rigorous derivation of quite a few results, in particular on quantum ground states. Second, the supersymmetric model turns out to have remarkable properties, both in dimension $D = 1$, where the model is quantum critical and described by a superconformal field theory [1–3], and in dimension $D = 2$, where the model displays extensive ground state entropy [4–6] and where indications of quantum critical behavior were found [7].

On the mathematics side the study of supersymmetric lattice models has led to interesting results on the cohomology of independence complexes of lattices and graphs, 2D grids in particular [8–14]. The two sides are connected by the observation that quantum ground states of the supersymmetric lattice model are in one-to-one correspondence with the elements of the cohomology of an associated independence complex.

The supersymmetric model on a 2D square lattice has turned out to be particularly interesting. Numerical results for the Witten index (Euler characteristic) in torus geometry led to remarkable conjectures for the dependence of this quantity on the two periods of the torus [15]. These conjectures were then proven by Jonsson [8], using a connection with specific rhombus tilings of the plane. In the present paper, we complete the analysis by providing a direct characterization of the elements of the cohomology and thereby of the quantum ground states for the square lattice wrapped around a torus. We prove a theorem, first conjectured by Fendley, which relates dimensions of the cohomology at grade n to the number of rhombus tilings with n rhombi. Since the number of rhombus tilings grows exponentially with the linear dimensions of the system, our result implies that the quantum model has a sub-extensive ground state entropy.

The presentation in this paper is organized as follows. In Section 2, we introduce the model and briefly summarize the main results presented in the literature so far. The focus in this section will be on the physics of the model. We then turn to the mathematics side in Section 3. We relate the Hilbert space of the supersymmetric lattice model to an independence complex and

show that the quantum ground states of the model are in one-to-one correspondence with the elements of the cohomology of this complex. At the end of this section, we resume the "tic-tac-toe" lemma of [16], which plays a central role in the rest of the paper. In Section 4, we state the main result of this paper; a theorem that relates the dimensions of the cohomology at grade n to the number of rhombus tilings with n rhombi. We briefly discuss how this theorem relates to Jonsson's work [8, 9] and what the implications for the physics of the model are. The remainder of the paper (Section 5) is dedicated to the proof of this theorem. Unfortunately, the proof is quite involved and consists of several steps. A detailed outline of these steps can be found at the start of Section 5.

2 Physics connection: supersymmetry and lattice fermions

In this section we will introduce the model and briefly state the main results obtained for this model with a focus on the physics interpretation.

2.1 Supersymmetry

An $\mathcal{N} = 2$ supersymmetric quantum mechanical theory is constructed from a basic algebra, defined by two nilpotent supercharges Q and $Q^\dagger$ (complex conjugation is implied) [17],

$$\{Q, Q\} = \{Q^\dagger, Q^\dagger\} = 0$$

and the Hamiltonian given by

$$H = \{Q^\dagger, Q\}.$$

It satisfies

$$[H, Q] = [H, Q^\dagger] = 0.$$

The eigenvalues and eigenvectors of the Hamiltonian give the energy spectrum and the corresponding quantum states. The definition of the Hamiltonian has some immediate consequences for the energy spectrum. First of all, it is positive definite:

$$\begin{aligned}\langle\psi|H|\psi\rangle &= \langle\psi|(Q^\dagger Q + QQ^\dagger)|\psi\rangle \\ &= |Q|\psi\rangle|^2 + |Q^\dagger|\psi\rangle|^2 \geq 0\end{aligned}$$

for all choices of the quantum state $|\psi\rangle$. Second of all, the fact that both Q and $Q^\dagger$ commute with the Hamiltonian, gives rise to a two-fold degeneracy in the energy spectrum. In other words, all eigenstates of the Hamiltonian with an energy $E_s > 0$ form doublet representations of the supersymmetry algebra. A doublet consists of two states, $|s\rangle$ and $Q|s\rangle$, such that $Q^\dagger|s\rangle = 0$. The states $|s\rangle$ and $Q|s\rangle$ are said to be superpartners. Finally, all states with zero energy must be singlets: $Q|g\rangle = Q^\dagger|g\rangle = 0$ and conversely, all singlets must be zero energy states [17]. In addition to supersymmetry our models will also have a particle-number symmetry generated by the operator F with

$$[F, Q^\dagger] = -Q^\dagger \quad \text{and} \quad [F, Q] = Q. \tag{2.1}$$

Consequently, F commutes with the Hamiltonian. Furthermore, this tells us that superpartners differ in their fermion number by one (let $F|s\rangle = f_s|s\rangle$, then $F(Q|s\rangle) = Q(F+1)|s\rangle = (f_s+1)(Q|s\rangle)$).

An important issue is whether or not supersymmetric ground states at zero energy occur, that is, whether there are singlet representations of the algebra. For this one considers the Witten index

$$W = \mathrm{tr}\Big[(-1)^F \mathrm{e}^{-\beta H}\Big], \tag{2.2}$$

where the trace is over the entire Hilbert space. Remember that all excited states come in doublets with the same energy and differing in their fermion number by one. This means that in the trace all contributions of excited states will cancel pairwise, and that the only states contributing are the zero energy ground states. We can thus evaluate W in the limit of $\beta \to 0$, where all states contribute $(-1)^F$. It also follows that $|W|$ is a lower bound to the number of zero energy ground states.

2.2 Lattice fermions

We now make the model more concrete by defining the supercharges in terms of lattice particles. The particles we will consider are spin-less electrons, also called spin-less fermions. Their key property is that the wavefunction is antisymmetric under the exchange of two fermions. It follows that the operator $c_i^\dagger$ that creates a fermion on site i in the lattice and the operator c_j that annihilates a fermion on site j in the lattice, satisfy the following

anti-commutation relations:

$$\{c_i^\dagger, c_j\} = \delta_{ij},$$
$$\{c_i, c_j\} = \{c_i^\dagger, c_j^\dagger\} = 0.$$

The particle-number operator for fermions is defined as $F = \sum_i c_i^\dagger c_i$, where the sum is over all lattice sites. This operator counts the total number of particles in a state. A simple choice for the supercharges would be $Q = \sum_i c_i^\dagger$ and $Q^\dagger = \sum_i c_i$. It is readily verified that both obey the nilpotency condition and that the commutation relations with F (2.1) are satisfied. However, this choice leads to a trivial Hamiltonian: $H = L$, where L is the total number of sites of the lattice. To obtain a non-trivial Hamiltonian, we dress the fermion with a projection operator: $P_{<i>} = \prod_{j \text{ next to } i}(1 - c_j^\dagger c_j)$, which requires all sites adjacent to site i to be empty. We can now formulate the supercharges in terms of these hard-core fermions: $Q = \sum c_i^\dagger P_{<i>}$ and $Q^\dagger = \sum c_i P_{<i>}$. Again the nilpotency condition and the commutation relations (2.1) are satisfied, but now the Hamiltonian of these hard-core fermions reads

$$H = \{Q^\dagger, Q\} = \sum_i \sum_{j \text{ next to } i} P_{<i>} c_i^\dagger c_j P_{<j>} + \sum_i P_{<i>}.$$

The first term is a nearest-neighbor hopping term, that is, the fermions can hop from site j to site i as long as i and j are connected by an edge and provided that the neighboring sites are empty. The second term contains a next-nearest-neighbor repulsion, a chemical potential and a constant. The details of the latter terms will depend on the lattice we choose.

2.3 Results and physics interpretation

This lattice Hamiltonian constitutes a particular instance of an itinerant-fermion system, where all the interactions are fine tuned by the supersymmetry. Over the last few decades, numerous studies of itinerant-fermion systems in two spatial dimensions have been presented, however, exact solutions are few and far between. The model presented here does allow for exact results and turns out to exhibit quite remarkable features. First of all, the supersymmetric model on the chain can be solved exactly through a Bethe ansatz [1]. In the continuum limit one can derive the thermodynamic Bethe ansatz equations. The model has the same thermodynamic equations as the XXZ chain at $\Delta = -1/2$, so the two models coincide (the mapping can be found in [2]). The continuum limit is described by the simplest field theory with $\mathcal{N} = (2, 2)$ superconformal symmetry with central charge $c = 1$,

which implies that the model is quantum critical. For a periodic chain with length $L = 3n$ the model has a twofold degenerate zero-energy ground state with $f = n$ fermions.

This ground state degeneracy turns out to be a generic feature of the model. In fact, in two spatial dimensions the ground state entropy S_{GS} typically grows exponentially with the system size. This characteristic of having an extensive ground state entropy goes under the name of superfrustration [4]. Numerical studies of the Witten index have shown that even this lower bound is typically extensive [5]. Exact results for the number of ground states were obtained for various lattices [4]. For example, for the martini lattice, which is formed by replacing every other site on a hexagonal lattice with a triangle, the number of zero-energy ground states $\mathrm{e}^{S_{\mathrm{GS}}}$ was found to equal the number of dimer coverings of the hexagonal lattice. For large systems ($L \to \infty$) this gives

$$\frac{S_{\mathrm{GS}}}{L} = \frac{1}{\pi} \int_0^{\pi/3} d\theta \ln[2\cos\theta] = 0.16153\ldots .$$

A heuristic way of understanding the superfrustration is from the "three-rule": to minimize the energy, fermions prefer to be mostly three sites apart (with details depending on the lattice). For generic two-dimensional lattices the three-rule can be satisfied in an exponential number of ways.

For certain two-dimensional lattices it was proven that zero-energy ground states exist at various fillings. The filling is defined as the number of particles per lattice site. For the square, triangular and hexagonal lattice there exist zero-energy ground states for all rational fillings ν within the range $[1/5, 1/4]$, $[1/7, 1/5]$ and $[1/4, 5/18]$, respectively [9].

The square lattice turns out to be a special case. Here the Witten index is subextensive and for periodic boundary conditions in two directions (i.e., the square lattice wrapped around the torus) it grows exponentially with the linear dimensions of the system [8, 15]. In this paper we prove that the total number of ground states also grows exponentially with the linear dimensions of the system. In fact, this proof establishes a direct relation between ground states and tilings of the plane with two types of rhombi (see Section 4 for details), which were first introduced by Jonsson. In [7] we presented numerical studies of various ladder realizations of the square lattice with doubly periodic boundary conditions. These studies, together with the correspondence between ground states and tilings, strongly indicate the existence of critical edge modes in these systems. It is compelling to infer that, if a subextensive systems accommodates edge criticality, a truly extensive system, like the triangular lattice, will allow for bulk criticality. On another

speculative note, the ground state-tiling correspondence for the square lattice on the torus suggests the possible existence of topological order in some of the many ground states.

3 Math connection: independence complex and cohomology theory

In this section we will establish the relation between particle configurations of hard-core fermions and independent sets, on the one hand, and between zero energy ground states and cohomology elements on the other. At the end of this section we state the "tic-tac-toe" lemma for double complexes, which plays a central role in the proof of the main result of this paper.

3.1 Independence complex

An independent set on a graph is a subset of the vertex set of the graph with the property that no two vertices are adjacent. Since hard-core fermions cannot occupy adjacent sites, it is clear that each allowed configuration of hard-core fermions forms an independent set. In the following, we will use the term lattice (i.e., a grid) instead of the more general term graph, since in the physics context it is most natural to study fermions on a lattice. However, the correspondences we establish in this section hold for graphs in general. The family of independent sets of a lattice forms the independence complex Σ of the lattice. We can define the partition sum in the asymptotic (thermodynamic) limit for the independence complex Σ as

$$Z(\Sigma, z) \equiv \sum_{\sigma \in \Sigma} z^{|\sigma|}, \tag{3.1}$$

where z is called the activity. Until recently there were essentially no exact results for independence complexes on two dimensional lattices, with one important exception. Baxter [18] gave an analytic expression for the partition sum of the independence complex on the triangular lattice with positive activity in the thermodynamic limit. This is also referred to as the exact solution for hard hexagons (hard-core fermions on the triangular lattice can, in this context, be viewed as hexagons that share, at most, a side or a corner).

Now observe that the coefficient of z^k in (3.1) is the number of sets in Σ with size k or, in other words, the number of configurations with k hard-core fermions. Consequently, $Z(\Sigma, 1)$ gives the dimension of the full Hilbert space $\mathcal{H}$; the space spanned by all possible hard-core fermion configurations. What is even more interesting, however, is that $Z(\Sigma, -1)$ coincides with the Witten index (2.2)

$$Z(\Sigma, -1) = \sum_{\sigma \in \Sigma} (-1)^{|\sigma|} = \mathrm{tr}(-1)^F.$$

Recently, Jonsson expressed precisely this quantity ($Z(\Sigma, -1)$) for hard squares on a torus, i.e., with doubly periodic boundary conditions, in terms of rhombus tilings on the torus [8] (see Section 4 for details). This quantity coincides with the Witten index for hard-core fermions on the square lattice. For the square lattice the condition that two particles cannot occupy two adjacent sites readily translates to the hard square condition if we define the squares to be tilted by 45° and to have a particle at their center. It follows that the squares cannot overlap; however, they can have a corner or a side in common.

3.2 Cohomology and homology theory

It should be clear from the previous that the Hilbert space is a graded vector space, where the grading is defined by the particle-number operator F. That is, the Hilbert space can be written as $\mathcal{H} = \oplus C_n$, where C_n is a subspace spanned by all the possible configurations with n particles. From the definitions of F and Q and their commutation relations (2.1) it is clear that Q is a map from C_n to C_{n+1}. Since Q squares to zero, we can define its cohomology. On the other hand, $Q^\dagger$ is a map from C_n to C_{n-1} and also nilpotent, so we can define the homology of $Q^\dagger$.

$$C_0 \underset{Q^\dagger}{\overset{Q}{\rightleftarrows}} C_1 \underset{Q^\dagger}{\overset{Q}{\rightleftarrows}} C_2 \underset{Q^\dagger}{\overset{Q}{\rightleftarrows}} C_3 \ldots$$

It turns out that the zero-energy ground states of the model are in one-to-one correspondence with the non-trivial classes of the cohomology of Q and the homology of $Q^\dagger$. Remember that all states with zero energy must be singlets: $Q|g\rangle = Q^\dagger|g\rangle = 0$ and conversely, all singlets must be zero-energy states. Clearly, all singlets, and thus all (zero-energy) ground states, are in the kernel of Q: $Q|g\rangle = 0$ and not in the image of Q, because if we could

write $|g\rangle = Q|f\rangle$, then $(|f\rangle, |g\rangle)$, would be a doublet. Equivalently, we can say that a ground state with n fermions is a cycle but not a boundary in C_n. This is precisely the definition of an element of the nth cohomology of Q, $H_Q^{(n)} = \ker Q/\mathrm{Im}\, Q$ within C_n. Two states $|s_1\rangle$ and $|s_2\rangle$ are said to be in the same cohomology class if $|s_1\rangle = |s_2\rangle + Q|s_3\rangle$ for some state $|s_3\rangle$. Since a ground state is annihilated by both Q and $Q^\dagger$, different (i.e., linearly independent) ground states must be in different cohomology classes of Q.[1] Finally, the number of independent ground states is precisely the dimension of the cohomology of Q and the fermion number of a ground state is the same as the grade of the corresponding cohomology class. Thus the ground states of a supersymmetric theory are in one-to-one correspondence with the cohomology of Q. With the same line of reasoning we may also conclude that the ground states are in one-to-one correspondence with the homology of $Q^\dagger$. Finally, the Euler characteristic, defined in cohomology theory as

$$\chi \equiv \sum_n \left[(-1)^n \dim H_Q^{(n)}\right],$$

is precisely the Witten index.

3.3 The "tic-tac-toe" lemma

Central to the proof presented in this paper is the "tic-tac-toe" lemma of [16]. Let us decompose the lattice S into two sublattices S_1 and $S_2 = S \setminus S_1$ and we write $Q = Q_1 + Q_2$, where Q_1 and Q_2 act on S_1 and S_2, respectively. We can then consider the double complex $\oplus_n C_n = \oplus_n \oplus_{p+q=n} K_{p,q}$, where p (q) is the size of the vertex set on S_1 (S_2). Equivalently, if we define f_i as the number of particles on S_i, we have $f_1 = p$ and $f_2 = q$. Finally, we have $Q_1 : K_{p,q} \to K_{p+1,q}$ and $Q_2 : K_{p,q} \to K_{p,q+1}$. The "tic-tac-toe" lemma now tells us that the cohomology of Q, H_Q, is the same as the cohomology of Q_1 acting on the cohomology of Q_2, i.e., $H_Q = H_{Q_1}(H_{Q_2}) \equiv H_{12}$, provided that H_{12} has entries only in one row. That is, H_{12} is non-vanishing only for

[1] Let $|s_1\rangle$ and $|s_2\rangle$ be two linearly independent ground states. It follows that $Q|s_1\rangle = Q|s_2\rangle = Q^\dagger|s_1\rangle = Q^\dagger|s_2\rangle = 0$. If we now write $|s_1\rangle = |s_2\rangle + Q|s_3\rangle$, we find that $Q^\dagger|s_1\rangle = Q^\dagger|s_2\rangle + Q^\dagger Q|s_3\rangle$ and thus $Q^\dagger Q|s_3\rangle = 0$. From this we find $\langle s_3|Q^\dagger Q|s_3\rangle = |Q|s_3\rangle|^2 = 0$ and thus $Q|s_3\rangle = 0$. With this we obtain $|s_1\rangle = |s_2\rangle$, which contradicts our assumption that $|s_1\rangle$ and $|s_2\rangle$ are linearly independent, so we conclude that $|s_1\rangle$ and $|s_2\rangle$ must be in different cohomology classes.

one value of q (or f_2).

$$\begin{array}{ccccccc}
\vdots & & \vdots & & \vdots & & \\
\uparrow Q_2 & & \uparrow Q_2 & & \uparrow Q_2 & & \\
K_{0,2} & \xrightarrow{Q_1} & K_{1,2} & \xrightarrow{Q_1} & K_{2,2} & \xrightarrow{Q_1} & \cdots \\
\uparrow Q_2 & & \uparrow Q_2 & & \uparrow Q_2 & & \\
K_{0,1} & \xrightarrow{Q_1} & K_{1,1} & \xrightarrow{Q_1} & K_{2,1} & \xrightarrow{Q_1} & \cdots \\
\uparrow Q_2 & & \uparrow Q_2 & & \uparrow Q_2 & & \\
K_{0,0} & \xrightarrow{Q_1} & K_{1,0} & \xrightarrow{Q_1} & K_{2,0} & \xrightarrow{Q_1} & \cdots
\end{array}$$

4 Statement of main result

The main result of this paper can be formulated both in the physics and mathematics context. We prove the result in the mathematics context, namely we find the dimensions of the cohomology for the independence complex on the square lattice wrapped around a torus. In the physics context this translates to the statement that we found the total number of ground states for the supersymmetric model on the square lattice wrapped around a torus. As we mentioned at the end of Section 2, the solution is found by relating ground states, or equivalently elements of the cohomology, to tilings of the plane with two types of rhombi. As was mentioned before, this relation is inspired by the work of Jonsson [8, 9]. He first introduced the rhombi when he related the partition sum of hard squares with activity $z = -1$ to these rhombus tilings. This is precisely the Witten index for our model on the square lattice, and also the Euler characteristic of H_Q. The Witten index is a lower bound to the number of ground states. The result we obtain in this paper gives us, not just this bound, but the total number of ground states with their respective fermion number in terms of rhombus tilings. A rhombus tiling is obtained by tiling the plane with the rhombi depicted in figure 1, such that the entire plane is tiled and the rhombi do not overlap (they can have only a corner or a side in common). We call the tiles with area four diamonds and the ones with area five squares. We can now state the main result of this paper.

Theorem 4.1. *For the square lattice with periodicities $\vec{v} = (v_1, v_2)$, $v_1 + v_2 = 3p$ with p a positive integer and $\vec{u} = (m, -m)$, we find for the cohomology H_Q*

$$N_n = \dim H_Q^{(n)} = t_n + \Delta_n, \tag{4.1}$$

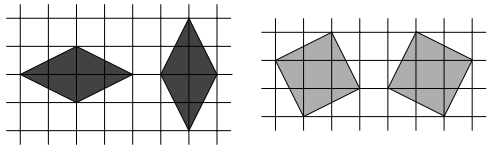

Figure 1: The diamonds on the left and squares on the right.

where N_n is the number of zero-energy ground states with n fermions, t_n is the number of rhombus tilings with n tiles, and

$$\Delta_n = \begin{cases} \Delta \equiv -(-1)^{(\theta_m+1)p}\theta_d\theta_{d*} & \textit{if } n = [2m/3]p, \\ 0 & \textit{otherwise,} \end{cases} \tag{4.2}$$

with $[a]$ the nearest integer to a. Finally, $d = \gcd(u_1 - u_2, v_1 - v_2)$, $d^* = \gcd(u_1 + u_2, v_1 + v_2)$ and

$$\theta_d \equiv \begin{cases} 2 & \textit{if } d = 3k, \textit{ with } k \textit{ integer}, \\ -1 & \textit{otherwise.} \end{cases} \tag{4.3}$$

As an immediate consequence of this theorem, we obtain for the Euler characteristic (=Witten index = $Z(\Sigma, -1)$)

$$\chi \equiv \sum_n \left[(-1)^n \dim H_Q^{(n)}\right] = \sum_n (-1)^n (t_n + \Delta_n).$$

which is precisely the result obtained by Jonsson for the hard squares at activity $z = -1$ [8].

Another direct consequence follows from the area of the tiles. The diamonds have area 4, and thus a tiling with solely diamonds will contain $L/4$ tiles. This corresponds to an element in the $(L/4)$th cohomology and a ground state with $L/4$ particles. Conversely, a tiling consisting of squares only corresponds to an element in the $(L/5)$th cohomology and a ground state with $L/5$ particles. Continuing this argument for general tilings with the diamonds and squares, we find on the infinite plane that for all rational numbers $r \in [\frac{1}{5}, \frac{1}{4}] \cap \mathbb{Q}$ the cohomology at grade rL is non-vanishing, or, equivalently, there exists a zero-energy ground state with rL particles. This result was obtained independently by Jonsson [9] for the homology of $Q^\dagger$. In fact, he found that for each tiling there is a so-called cross-cycle, which is a representative of the homology of $Q^\dagger$. However, he could not prove that these cross-cycles are independent, i.e., in different homology classes, nor that they

constitute a basis. A comparison with our result, Theorem 4.1, suggests that the cross-cycles are indeed independent and span the full homology with the exception of Δ_n elements at the nth grade.

Finally, the theorem provides insight in the growth behavior of the number of ground states, since this is now directly related to the growth behavior of the number of tilings. In [10] various results on the number of tilings on the doubly periodic square lattice are reported. Here we mention two of these results for the case that $\vec{u} = (m, -m)$ and $\vec{v} = (k, k)$.

1. For m and k such that $\gcd(m, k) = 1$, there are no rhombus tilings that satisfy the periodicities given by $\vec{u}$ and $\vec{v}$.
2. For $m = 3\mu r$ and $k = 3\lambda r$, with μ and λ positive integers and r large, the total number of rhombus tilings t grows as

$$t \equiv \sum_n t_n \sim \frac{9}{2} \frac{4^{\mu r + \lambda r}}{\pi r \sqrt{\mu\lambda}}.$$

In the first case it follows that the number of ground states with n particles is given by Δ_n, which is non-zero only for $n = [2m/3]p$ given that $2k = 3p$. In the second case the number of ground states will show the same growth behavior as the number of tilings. This number turns out to be dominated entirely by the number of tilings with $2L/9$ tiles. Furthermore, it is noteworthy that the number of tilings grows exponentially with the linear dimensions, instead of the area, of the system. It follows that, eventhough the system is highly frustrated, this leads only to a sub-extensive ground state entropy. This is in contrast with results obtained for the triangular, hexagonal and martini lattices, for which the ground state entropy was found to be extensive [4, 5].

5 Proof of main result

In this section we present the proof of Theorem 4.1. Unfortunately, the proof is quite involved and consists of several intermediate steps. Here we will give a brief outline of these steps. In Section 3.3 we resumed the "tic-tac-toe" lemma which plays a crucial role in the proof. The lemma relates H_Q to H_{Q_1} and H_{Q_2} when Q is written as $Q_1 + Q_2$. This is achieved by writing the lattice S as $S_1 \cup S_2$ and letting Q_i act solely on S_i. The crucial step is to choose the right sublattices. It turns out that for the square lattice one should pick a set of disconnected points for S_1 and a set of (disconnected) chains for S_2 (for the details see Definition 5.2).

First, in Section 5.1, we will discuss the cohomology results for a single chain with various boundary conditions. These results are crucial in the first step of the "tic-tac-toe" lemma, i.e., computing the cohomology of Q_2, since Q_2 acts on a set of chains.

Second, in Section 5.2, we consider the square lattice on the plane and on the cylinder, to illustrate the power of the "tic-tac-toe" lemma for a relatively simple case. We choose the boundary conditions in such a way that H_{Q_2} is non-vanishing only for one value of f_1 and f_2. Consequently, H_{12} and H_Q are trivially obtained from H_{Q_2}.

Finally, we wrap the square lattice around the torus. We then apply the same strategy as in Section 5.2, and H_{Q_2} is easily obtained. Unfortunately, however, it has entries in several rows and columns of the double complex and computing H_{12} is highly non-trivial.

As a first step (Section 5.3.1), we compute H_{12} for a thin torus, such that the S_2 sublattice consists of one chain only. For this case, we then show that $H_Q = H_{12}$, even though H_{12} has entries in multiple rows. The final step for this simple case is to relate the elements of H_Q to periodic sequences of tiles and identify the elements that give rise to the small number Δ in (4.1).

In the last step (Section 5.3.2), we finally present the proof of Theorem 4.1. Here the sublattice S_2 consists of an arbitrary number of chains. We proceed as in Section 5.3.1 to obtain H_{12} and each step will be similar, but slightly more involved. Again we find that H_{12} does not have entries only in one row. In contrast to the thin torus case, however, we find that here H_Q is contained in but not equal to H_{12}. Using the "tic-tac-toe" procedure, we reduce H_{12} to obtain H_Q. What we find is that all the elements of H_Q can be obtained by concatenating so-called building blocks and in the final step we map each building block to a sequence of tiles. It follows from this mapping, that the elements of H_Q map to all possible tilings, again with a small discrepancy Δ, which is computed in the very last step.

5.1 The cohomology of Q on the chain

In the following sections, we will often use the cohomology results for the supersymmetric model on the chain. These results can be found in [1, 2], but will be restated here for completeness.

Definition 5.1. An open chain of length L is the graph $G(V, E)$ with vertices $V = \{v_j | j \in \mathbb{N}, j \leq L\}$ and edges $E = \{(v_j, v_{j+1}) | j \in \mathbb{N}, j < L\}$. A

periodic chain of length L is a cycle defined by the graph $G(V, E')$ where $E' = E \cup \{(v_L, v_1)\}$.

In the following, $j \in \mathbb{N}$ (j can also be zero as long as the number of sites L is positive).

Theorem 5.1. *The cohomology of Q on the periodic chain with L sites has:*

- *two non-trivial cohomology classes with j fermions if $L = 3j$,*
- *one non-trivial cohomology class with j fermions if $L = 3j \pm 1$.*

The cohomology of Q on the open chain with L sites has:

- *one non-trivial cohomology class with j fermions if $L = 3j$ or $L = 3j - 1$,*
- *zero non-trivial cohomology classes if $L = 3j + 1$.*

Proof. We prove this result for the periodic chain with $L = 3j$ sites. We take S_2 to be every third site and the remaining sites S_1. Remember that f_i is the number of fermions on sublattice S_i. Consider a single site on S_2. If both of the adjacent S_1 sites are empty, H_{Q_2} is trivial: Q_2 acting on the empty site does not vanish, while the filled site is Q_2 acting on the empty site. So the empty site does not belong to the kernel of Q_2, whereas the filled site belongs to the image of Q_2. This leads to a vanishing H_{Q_2}, unless every site on S_2 is forced to be empty by being adjacent to an occupied site. There are only two such configurations:

$$\begin{aligned} |\alpha\rangle &\equiv \cdots \bullet\,\square\,\circ\,\bullet\square\,\circ\,\bullet\square\,\circ\,\bullet\square\,\circ\,\bullet\square\,\circ\,\bullet\square\,\circ\,\bullet\square\,\circ\ldots \\ |\gamma\rangle &\equiv \cdots \circ\,\square\,\bullet\,\circ\square\,\bullet\,\circ\square\,\bullet\,\circ\square\,\bullet\,\circ\square\,\bullet\,\circ\square\,\bullet\,\circ\square\,\bullet\ldots \end{aligned} \tag{5.1}$$

where the square represents an empty site on S_2. Both states $|\alpha\rangle$ and $|\gamma\rangle$ belong to H_{12}: they are closed because $Q_1|\alpha\rangle = Q_1|\gamma\rangle = 0$, and not exact because there are no elements of H_{Q_2} with $f_1 = f - 1$ fermions, where $f = L/3 = j$. By the "tic-tac-toe" lemma, there must be precisely two different cohomology classes in H_Q, and therefore exactly two ground states with j fermions. $\square$

The proofs for the other cases are completely analogous. In the main proof we will need the representatives of the non-trivial cohomology classes of Q on the open chain. We will use the following notation: to denote a configuration with fermions on sites a, b, c, etc. we write $|a, b, c \ldots\rangle$.

Lemma 5.1. *A representative of the non-trivial cohomology classes of Q on the open chain with $L = 3j$ or $L = 3j - 1$ sites is*

$$|\phi\rangle \equiv |2, 5, 8 \ldots 3j - 1\rangle, \tag{5.2}$$

where on the dots the numbers always increase by three.

Proof. From Theorem 5.1 we know that the representative has j fermions. In the case that $L = 3j$ it follows that $|\phi\rangle$ is the only configuration with j fermions that belongs to the kernel of Q. Since the dimension of H_Q is one, $|\phi\rangle$ must be a representative of the non-trivial cohomology class.

When $L = 3j - 1$ there are two configurations that belong to the kernel of Q: $|1, 4, 7 \ldots 3j - 2\rangle$ and $|2, 5, 8 \ldots 3j - 1\rangle$, however the dimension of H_Q is again just one. It follows that a linear combination of these two configurations will be in the image of Q. In general, two states $|s_1\rangle$ and $|s_2\rangle$ are in the same cohomology class if one can write $|s_1\rangle = |s_2\rangle + Q|s_3\rangle$ for some state $|s_3\rangle$. In that case both $|s_1\rangle$ and $|s_2\rangle$ are good representatives of the cohomology class. Since $|\phi\rangle$ itself is not in the image of Q it is thus a good representative. □

5.2 The cohomology of Q on the square lattice. Part I: Tilted rectangles and cylinders

Let us define $\mathcal{R}(M, N)$ with $M, N \geq 1$ as the subset of $\mathbb{Z}^2$ given by the points (x, y) such that

$$y \leq x \leq y + M - 1 \quad \text{and} \quad -y + 1 \leq x \leq -y + N. \tag{5.3}$$

This defines a tilted rectangular part of the square lattice. We can also define $\tilde{\mathcal{R}}(M, N)$ with $M, N \geq 1$ as the subset of $\mathbb{Z}^2$ given by the points (x, y) such that

$$y \leq x \leq y + M - 1 \quad \text{and} \quad -y \leq x \leq -y + N - 1. \tag{5.4}$$

Whereas $\tilde{\mathcal{R}}(M, N)$ contains the point $(0, 0)$, it is excluded in $\mathcal{R}(M, N)$. The lattice $\tilde{\mathcal{R}}(M, N)$ can be mapped to a lattice of the former type except when M and N are both odd. Finally, for M even the cylindrical version $\mathcal{R}_{\mathrm{c}}(M, N)$ can be obtained from $\mathcal{R}(M + 1, N)$ by identifying the vertices (i, i) and $(i + M/2, i - M/2)$.

For the lattices $\mathcal{R}(M, N)$, $\tilde{\mathcal{R}}(M, N)$ and $\mathcal{R}_{\mathrm{c}}(M, N)$ the full cohomology problem has been solved using Morse theory [12]. These cases can also be

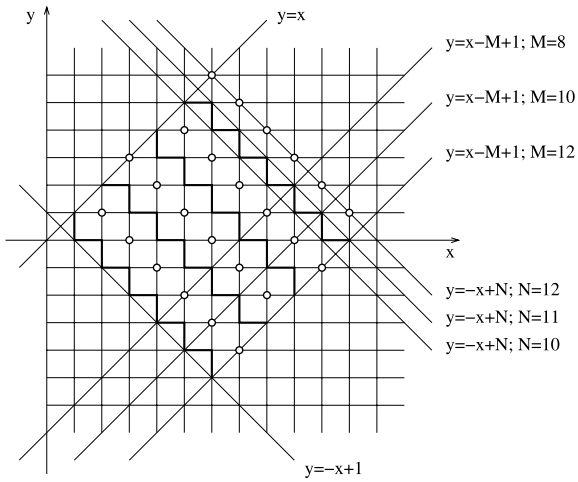

Figure 2: Sublattice S_1 is indicated by circles and sublattice S_2 is indicated by the fat lines. The bounding lines of $\mathcal{R}(M,N)$ defined in (5.3) are drawn for various values of M and N. For the cylinder M should be even, but for the rectangle it can be odd as well. One easily checks that the length of the S_2 chain is M. Note that for $N = 3n+1$ only half of the upper-right S_2 chain is included in $\mathcal{R}(M,N)$.

solved using the "tic-tac-toe" lemma. The crucial step is to choose the right sublattices. We take a set of disconnected sites for S_1 and a set of (open or periodic) chains for S_2 (see figure 2).

Definition 5.2. More formally, for $\mathcal{R}(M,N)$ S_1 is the set of points (x,y) that satisfy

$$\begin{aligned} &y \le x \le y+M-1 \quad \text{and} \quad -y \le x \le -y+N-1 \\ &\quad \text{and} \quad x = -y+3s, \end{aligned} \tag{5.5}$$

with $3 \le 3s \le N-1$ and S_2 is the set of points (x,y) that satisfy

$$\begin{aligned} &y \le x \le y+M-1 \quad \text{and} \quad -y \le x \le -y+N-1 \\ &\quad \text{and} \quad -y+3p+1 \le x \le -y+3p+2, \end{aligned} \tag{5.6}$$

with $0 \le 3p \le N-3$. The sublattices can be defined similarly for $\tilde{\mathcal{R}}(M,N)$.

To solve H_{Q_2} we start from the bottom-left chain. If a site on S_1 directly above this chain is occupied, we are left with an isolated site on the bottom-left chain (see figure 3), leading to a vanishing H_{Q_2} (see Section 5.1). It follows that all sites directly above the bottom-left chain must be empty.

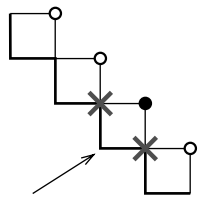

Figure 3: A site directly above the bottom-left chain is occupied. This generates an isolated site on the bottom-left chain.

Continuing this argument for subsequent chains one finds that all sites on S_1 must be empty. However, in the case that $N = 3l + 1$ we have a set of disconnected sites at the top-right that belong to S_2. From the previous argument we obtained that the sites of S_1 directly below the top-right sites of S_2 have to be empty. This implies that for $N = 3l + 1$ H_{Q_2} vanishes. When $N \neq 3l + 1$ we find that all elements in H_{Q_2} have all sites in S_1 empty, thus computing $H_{Q_1}(H_{Q_2})$ is a trivial step. The dimension of H_Q is related to the number of ground states, or equivalently, the number of non-trivial cohomology classes of Q on the chains that constitute S_2. Note that the length of these chains is M both for the tilted rectangles as well as for the cylinder. In the first case the chains have open boundary conditions, whereas in the latter the chains are periodic. Now, the number of non-trivial cohomology classes of Q for all these cases can be found in Theorem 5.1.

It follows that for the tilted rectangles, $\mathcal{R}(M, N)$ and $\tilde{\mathcal{R}}(M, N)$, with $N \neq 3l + 1$ we have

(i) no non-trivial cohomology classes for $M = 3p + 1$ and
(ii) one non-trivial cohomology class for $M \neq 3p + 1$.

For the cylinder, $\mathcal{R}_{\mathrm{c}}(M, N)$, with $N \neq 3l + 1$ and M even we have

(i) one non-trivial cohomology class for $M = 3p \pm 1$
(ii) 2^K non-trivial cohomology classes for $M = 3p$, with K the nearest integer to $N/3$.

For $N = 3l + 1$ the non-trivial cohomology vanishes for both the rectangle and the cylinder.

5.3 The cohomology of Q on the square lattice. Part II: The torus

We now define the doubly periodic lattices via two linearly independent vectors $\vec{u} = (u_1, u_2)$ and $\vec{v} = (v_1, v_2)$. We wrap the square lattice around the torus by identifying all points (i, j) with $(i + ku_1 + lv_1, j + ku_2 + lv_2)$.

The main result of this paper is that we find the full cohomology of Q on the square lattice with doubly periodic boundary conditions defined by $\vec{u} = (m, -m)$ and $\vec{v} = (v_1, v_2)$ such that $v_1 + v_2 = 3p$. In particular, we obtain a direct relation between elements of H_Q and tiling configurations. This relation allows us to prove Theorem 4.1, that was first conjectured by Fendley and is strongly inspired by the work of Jonsson [8, 9]. It is restated here for convenience.

For the square lattice with periodicities $\vec{v} = (v_1, v_2)$, $v_1 + v_2 = 3p$ with p a positive integer and $\vec{u} = (m, -m)$, we find for the cohomology H_Q

$$N_n = \dim H_Q^{(n)} = t_n + \Delta_n$$

where N_n is the number of zero energy ground states with n fermions, t_n is the number of rhombus tilings with n tiles, and

$$\Delta_n = \begin{cases} \Delta \equiv -(-1)^{(\theta_m+1)p}\theta_d\theta_{d*} & \text{if } n = [2m/3]p, \\ 0 & \text{otherwise,} \end{cases}$$

with $[a]$ the nearest integer to a. Finally, $d = \gcd(u_1 - u_2, v_1 - v_2)$, $d^* = \gcd(u_1 + u_2, v_1 + v_2)$ and

$$\theta_d \equiv \begin{cases} 2 & \text{if } d = 3k, \text{ with } k \text{ integer,} \\ -1 & \text{otherwise.} \end{cases}$$

Computing the cohomology for these tori is far from trivial. First of all, computing H_{Q_2} does not imply that all sites on S_1 are empty, instead there are many allowed configurations on S_1. Secondly, because of this, computing $H_{Q_1}(H_{Q_2})$ becomes much more involved. Finally, we will see that, generally, H_Q will be contained in H_{12}, but not equal to H_{12}.

We will divide the proof into two parts. We start by proving the theorem for a specific torus, defined by $\vec{u} = (m, -m)$ and $\vec{v} = (1, 2)$. This proof will already contain many steps that we use in the proof for the more general case, however, it will be deprived of certain complications. For instance, here we will find $H_Q = H_{12}$. As we said, this is not true in general, and in the second part of the proof a substantial part will be concerned with obtaining H_Q once we have found H_{12}.

5.3.1 A special case: S_2 consisting of one chain

In this section we consider the case where $\vec{v} = (1, 2)$ and $\vec{u} = (m, -m)$. It follows that S_2 consists of exactly one periodic chain (see figure 4).

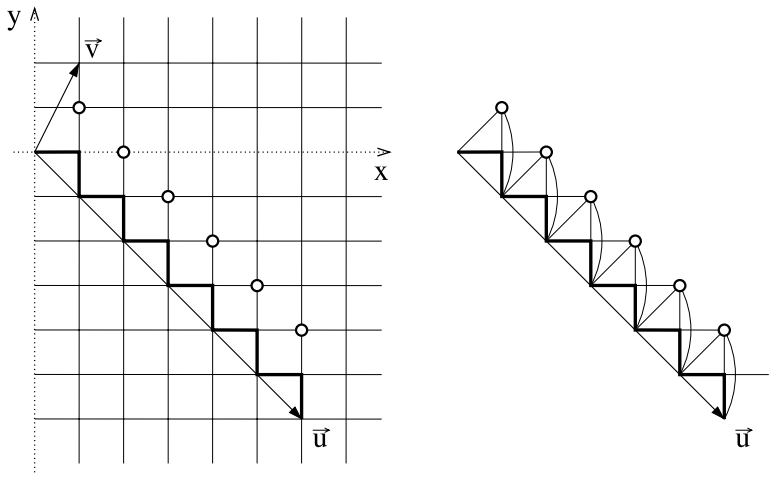

Figure 4: The square lattice is wrapped around the torus by imposing periodicities $\vec{v}$ and $\vec{u}$. Here $\vec{v} = (1, 2)$ and $\vec{u} = (m, -m)$, consequently S_2 consists of one chain. On the right we have drawn the cylinder, where periodicity in the $\vec{u}$-direction is still implied.

The proof of Theorem 4.1 for this case will consist of four steps:

1. We compute H_{Q_2}.
2. We compute $H_{12} = H_{Q_1}(H_{Q_2})$ and show that its elements can be constructed from a finite number of building blocks, called motifs. A motif is characterized by a certain configuration on a finite number of subsequent S_1 sites.
3. We show that $H_Q = H_{12}$.
4. We relate the elements of H_Q to tiling configurations by relating each motif to a small series of tiles.

Step 1. First we compute H_{Q_2} and we find the following:

Lemma 5.2. *The cohomology of Q_2 consists of all possible configurations on S_1 except for configurations with a multiple of three S_1 sites empty between two occupied S_1 sites.*

Proof. The proof is relatively simple. First note that when a site on S_1 is occupied, it blocks four subsequent sites on the S_2 chain (see figure 4). By occupying sites on S_1 the periodic S_2 chain is cut into smaller pieces of chain with open boundary conditions. Consequently, H_{Q_2} vanishes when at least one of these smaller pieces has length $3p + 1$. This happens when the number of empty sites between two occupied sites on S_1 is a multiple of three. We conclude that all configurations on S_1 are allowed except for

configurations with a multiple of three sites empty between two occupied sites. □

Step 2. This step in the proof is the most involved. In the next section, where we prove Theorem 4.1 in all generality, we will often refer back to the results obtained in this step. In this step we compute $H_{Q_1}(H_{Q_2})$, where H_{Q_2} was obtained in the previous step. Let us define f_1 and f_2 as the number of fermions on S_1 and S_2, respectively. Furthermore, we shall adopt the following notation: an empty site on S_1 is denoted by 0 and an occupied site is denoted by 1. A configuration on S_1 can then be written as a series of 1's and 0's. In the following, we shall consider all possible types of configurations on S_1 that belong to H_{Q_2} and we shall investigate if they also belong to H_{12}.

If we consider a configuration on S_1, we note that there have to be at least two adjacent, empty S_1 sites to allow for $f_2 > 0$. This is because two adjacent empty sites leave an open chain of two sites unblocked on S_2 and this has an element in H_{Q_2} with $f_2 = 1$. A typical configuration will thus consist of alternating segments, where a segment is a sequence of S_1 sites. The segments are characterized by the number of fermions on the part of the S_2 chain corresponding to the segment, this is either zero or greater than zero. In a segment with $f_2 > 0$ all S_1 sites are empty and it contains at least two sites. On the other hand, a segment with $f_2 = 0$ can have empty sites on S_1, but the empty sites cannot be adjacent. Finally, a segment with $f_2 = 0$ will always start and end with an occupied S_1 site. We will call this pair of occupied sites a pair of bounding sites. Note that a segment with $f_2 = 0$ can consist of a single occupied site, in that case the bounding sites fall on top of each other and the pair of bounding sites is just this one site.

Example 5.1. Consider the configuration "1101101010000100", there are two segments with $f_2 = 0$, formed by the first nine sites and the 14th site, respectively. There are also two segments with $f_2 > 0$ constituted by the rest of the sites. Finally, the first and the ninth site form a pair of bounding sites.

First, we consider the segments with $f_2 > 0$.

Lemma 5.3. *Q_1 acting on a segment with $f_2 > 0$ gives zero within H_{Q_2}.*

Proof. Suppose this segment between a pair of bounding sites consists of l empty S_1 sites. The corresponding S_2 chain then has length $L = 2l - 2$. Since $l = 3k \pm 1$, we find $L = 6k$ or $L = 6k - 4$. For these chain lengths the elements of the cohomology of Q_2 have $2k$ and $2k - 1$ fermions, respectively. We now distinguish two cases: (a) Q_1 acts on a site at the boundary of the segment and (b) Q_1 acts on a site away from the boundary.

(a) In this case the length of the S_2 chain in the new configuration is $L' = L - 2$. Thus $L' = 6k - 2$ or $L' = 6k - 6$. On the new chain there are still $2k$ or $2k - 1$ fermions, respectively. However, Theorem 5.1 states that the cohomology for chain length $6k - 2$ ($6k - 6$) vanishes at all fermion numbers except $f = 2k - 1$ ($f = 2k - 2$). Thus the new configuration does not belong to H_{Q_2} and it follows that this action of Q_1 within H_{Q_2} gives zero.

(b) In this case the action of Q_1 cuts the S_2 chain into two smaller chains of lengths L'_1 and L'_2. Their total length is $L'_1 + L'_2 = L - 4$, since the occupied S_1 site now blocks four sites on the S_2 chain. For $L = 6k$ we have $L'_1 = 3k_1$ and $L'_2 = 3k_2 + 2$ or $L'_1 = 3k_1 + 1$ and $L'_2 = 3k_2 + 1$, where in both cases $k_1 + k_2 = 2k - 2$. For the latter case H_{Q_2} vanishes at all grades. In the first case H_{Q_2} is non-vanishing only for $f = k_1 + k_2 + 1 = 2k - 1$. However, the number of fermions on the S_2 chains in the new configuration is $f = 2k$ and thus is does not belong to H_{Q_2}. Similarly, one finds that for $L = 6k - 4$, the new configuration does not belong to H_{Q_2}. Again we obtain that this action of Q_1 within H_{Q_2} gives zero.

Finally, if the segment with $f_2 > 0$ extends over the entire system, we are always in the case considered under (b). However, the original chain length can now also be $L = 6k - 2$ with $2k - 1$ fermions on it. Under the action of Q_1 we obtain a new chain of length $L' = 6k - 6$, which has a non-vanishing cohomology if and only if $f = 2k - 2$. So also in this case we find that the action of Q_1 gives zero within H_{Q_2}. □

Second, we consider the segments with $f_2 = 0$.

Lemma 5.4. *$H_{Q_1}(H_{Q_2})$ vanishes when the number of S_1 sites between any pair of bounding sites in a segment with $f_2 = 0$, is $3p + 1$ and it contains one element otherwise.*

Example 5.2. Consider a configuration with one empty site between a pair of bounding sites: "101," this is not an element of $H_{Q_1}(H_{Q_2})$, since Q_1 on this configuration gives "111," which is also in H_{Q_2}. Now consider two sites between a pair of bounding sites. Then there are two configuration with one empty site: "1011" and "1101" and one configuration with all sites occupied "1111" (remember that the configuration "1001" does not have $f_2 = 0$). It follows that Q_1 acting on ("1101" − "1011") gives 2"1111," whereas Q_1 acting on ("1101" + "1011") gives zero.[2] Consequently, we find

[2]Note that the fermionic character of the particles is reflected in the sign here: Q_1 acting on "1011" gives −"1111," whereas Q_1 acting on "1101" gives +"1111". In the first case the particle is created on position 2 and has to hop over the particle at position 1, this gives a minus sign, in the second case the new particle is created at position 3 and

that $H_{Q_1}(H_{Q_2})$ consists of one element: the sum of the configurations with $f_1 = 3$.

Proof. We can solve $H_{Q_1}(H_{Q_2})$ for an arbitrary number of sites between a pair of bounding sites, by realizing that this problem can be mapped to the normal chain. For the normal chain no two fermions can be adjacent, whereas here no two empty S_1 sites can be adjacent. So we can map empty S_1 sites to fermions on the chain and occupied S_1 sites to empty sites in the normal chain. Finally, Q_1 is mapped to $Q^\dagger$ on the normal chain. For the chain $H_{Q^\dagger}$ (which has the same dimension as H_Q) vanishes when the length of the chain is $3p+1$ and it contains one element otherwise. So here we have that $H_{Q_1}(H_{Q_2})$ vanishes when the number of sites between two occupied sites is $3p+1$ and it contains one element otherwise. □

For a segment with $f_2 = 0$, let us denote the representative of $H_{Q_1}(H_{Q_2})$ by the pair of bounding sites with dots in between, for example we denote ("1101" + "1011") by "$1 \cdot\cdot 1$." Even though, this is now a sum of configurations, we will still refer to this simply as a configuration. It follows that, for a segment with $f_2 = 0$, two types of configurations are allowed. The two types can be distinguished by containing $3s-1$ dots or $3s$ dots. Examples of the first type are: "1", "$1 \cdot\cdot 1$", "$1 \cdot\cdot\cdot\cdot\cdot 1$," etc. Note that the configuration with $s = 0$, and thus with -1 dots between the pair of bounding sites, is "1." Examples of the second type are: "11," "$1 \cdot\cdot\cdot 1$," "$1 \cdot\cdot\cdot\cdot\cdot\cdot 1$," etc.

Combining Lemmas 5.3 and 5.4, we find that $H_{Q_1}(H_{Q_2})$ is spanned by all configurations that can be formed by concatenating the following motifs:
"000",
"$1 \cdot_{3s-1} 100$",
"$1 \cdot_{3s} 100$",
"$1 \cdot_{3s-1} 10000$",
"$1 \cdot_{3s} 10000$",
where $\cdot_{3s}$ means $3s$ dots and, as before, "$1 \cdot_{3s-1} 1$" with $s = 0$ means "1".

Finally, one can also have all zeroes for any length and all dots for any length. Note that if the number of S_1 sites is a multiple of three, that both the configuration with all zeroes and the one with all dots account for two linearly independent elements of H_{12}. This is because the cohomology of Q acting the periodic chain with length a multiple of three has dimension two (see Theorem 5.1).

thus has to hop over two particles, giving rise to no overall sign change. Also note that the states are not properly normalized, but this is not important for the argument.

Example 5.3. As an example, suppose we have $\vec{v} = (1, 2)$ as always and $\vec{u} = (10, -10)$. This implies that S_1 consists of ten sites and with the defined motifs it follows that the following 12 elements belong to H_{12}: "1100000000," "1100000100," "1100100000," "1100100100," "1100110000," "1100 1 · ·100," "1 · · · · · ·100," "1 · · · 100 000," "1 · · · 100 100," "1000010000," "0000000000" and "· · · · · · · · · ·." Note that the first nine motifs have periodicity 10 and thus account for ten elements of H_{12} each, whereas the motif "1000010000" has periodicity 5 and the last two motifs have periodicity 1. For each element one can easily compute the number of fermions and it follows that the first nine motifs have nine fermions, the motif "1000010000" has six fermions and the last two motifs have again seven fermions. So in total we have 92 elements in H_{12} with seven fermions and five elements with six fermions.

Step 3. In the previous step we have obtained H_{12} for $\vec{v} = (1, 2)$. In this step we show that in this case this is equal to the cohomology of Q. We do this via the "tic-tac-toe" procedure [16]. That is, we act on a configuration, say $|\psi\rangle$, with Q. The Q_2 part will automatically give zero, but the Q_1 part not necessarily, since we no longer restrict ourselves to the subspace H_{Q_2}. If it does give zero, we know that the configuration belongs to the kernel of Q. The configuration will thus belong to H_Q unless it also belongs to the image of Q. In that case, another configuration will map to this configuration at the end of the "tic-tac-toe" procedure. So we continue with the configurations, $|\psi_0\rangle$, that do not belong to the kernel of Q_1. Since the image of $|\psi_0\rangle$ does not belong to H_{Q_2} and it does belong to the kernel of Q_2, it must also belong to the image of Q_2. So we can write $Q|\psi_0\rangle = Q_2|\phi\rangle$, for some configuration $|\phi\rangle$. Now let us define a new state $|\psi_1\rangle \equiv |\psi_0\rangle - |\phi\rangle$. It then follows that $Q|\psi_1\rangle = -Q_1|\phi\rangle$. If this is zero, we have found that the state $|\psi_1\rangle$ belongs to the kernel of Q. If it is non-zero we proceed as before: we try to find a configuration $|\chi\rangle$, such that $Q_1|\phi\rangle = Q_2|\chi\rangle$ and define a new state $|\psi_2\rangle \equiv |\psi_0\rangle - |\phi\rangle + |\chi\rangle$, etc. This procedure ends, either when we have found a state $|\psi_n\rangle$ such that $Q|\psi_n\rangle = 0$, or when $Q|\psi_n\rangle = |\tilde{\psi}\rangle$ with $|\tilde{\psi}\rangle$ an element of $H_{Q_1}(H_{Q_2})$. In the latter case, we say $|\psi_0\rangle$ maps to $|\tilde{\psi}\rangle$ at the end of the "tic-tac-toe" procedure and we conclude that neither $|\psi_0\rangle$ nor $|\tilde{\psi}\rangle$ belong to H_Q.

For the case we consider in this section, we will show that for each element $|\psi_0\rangle$, there is an element $|\psi_n\rangle$ that belongs to the kernel of Q. So for each element in H_{12} we can find a corresponding element in H_Q, thus we obtain $H_Q = H_{12}$. In the next section, however, we will see that this is not true for general boundary conditions. We will then find that after several steps in the "tic-tac-toe" procedure we map certain configurations in H_{12} to other configurations in H_{12}. It follows that the first do not belong to the kernel

of Q and the latter belong to the image of Q. In that case H_Q is strictly smaller than H_{12}.

Lemma 5.5. *$H_Q = H_{12}$ for $\vec{v} = (1,2)$ and $\vec{u} = (m,-m)$.*

Proof. For the segments with $f_2 = 0$, we found that Q_1 vanishes if we choose the states represented by the dots such that they are ground states of the normal chain with empty and occupied sites exchanged (see Lemma 5.4). For the segments with $f_2 > 0$, we know from Lemma 5.3 that the new configuration always belongs to the image of Q_2. That is, $Q_1|\psi_0\rangle = Q_2|\phi\rangle$, for some configuration $|\phi\rangle$ if Q_1 acts on a segment with $f_2 > 0$. So we can define a new configuration $|\psi_1\rangle \equiv |\psi_0\rangle - |\phi\rangle$, such that $Q|\psi_1\rangle = -Q_1|\phi\rangle$. Now Q_1 either acts on a different segment with $f_2 > 0$, in which case the new configuration again belongs to the image of Q_2, or it acts on the same segment. In the latter case, the new configuration is cancelled by the same configuration in which the two S_1 sites are occupied in the reverse order due to the fermionic character of the particles. It thus follows that the "tic-tac-toe" procedure always gives zero after as many steps as there are segments with $f_2 > 0$. □

Step 4. In this final step we will show that the dimension of H_Q (and the fermion number of each state) can be computed by counting all tiling configurations (and the number of tiles per configuration) with the four types of tiles depicted in figure 1. For the boundary conditions we consider here, the tilings reduce to a single layer sequence of only two types of tiles. Namely, the two tiles that respect the boundary condition $\vec{v} = (1,2)$. These tiles have two edges parallel to $(1,2)$ and then the diamond has the other two edges parallel to $(1,-2)$ whereas the square has the other edges parallel to $(2,-1)$ (see figure 5(a)). Given the sublattices S_1 and S_2 there are three types of vertices: the ones that belong to S_1, the lower left sites of the S_2-chain and the upper right sites of the S_2 chain. It follows that the diamond has one of three types of edges along the $(1,-2)$ direction and a matching type of edge along the $(1,2)$ direction, the square can have one of three different types of edges along the $(2,-1)$ direction and a matching type of edge along the $(1,2)$ direction. We conclude that we have six types of tiles, depicted in figure 5(b).

To establish Theorem 4.1 we map each of the motifs obtained in step 2 to a unique sequence of tiles. The mapping for the four basis motifs, "100," "1100," "10000" and "110000," is shown in figure 6. Remember that each motif is modulo the addition of three zeroes and modulo the insertion of three dots. In terms of tilings, we find that each basis motif can be followed by an arbitrary repetition of the tiling corresponding to the three zeroes

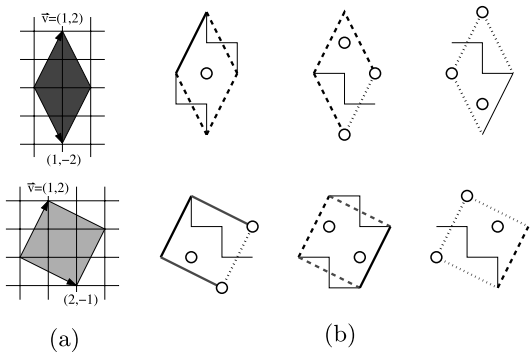

Figure 5: Types of tiles we use to tile the square lattice with periodicities $\vec{v} = (1, 2)$ and $\vec{u} = (m, -m)$. (a) Shows the diamond and square that respect $\vec{v} = (1, 2)$. (b) Shows the three types of diamonds and squares given the sublattices S_1 and S_2.

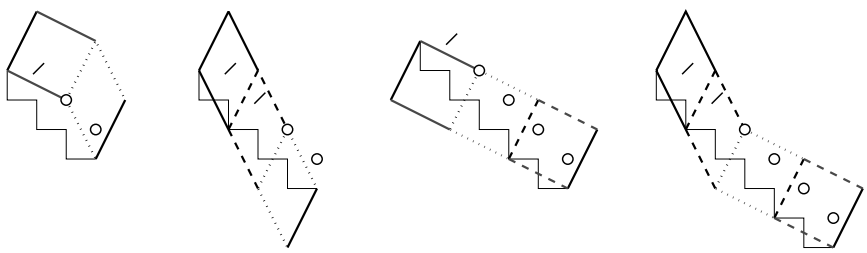

Figure 6: The four basis motifs and the corresponding sequences of tiles.

(see figure 7(a)). On the other hand, insertions of multiples of three dots correspond to inserting multiples of the tiling shown in figure 7(a) at the dotted line along the $(1, 2)$ direction in the basis motifs. Some examples are shown in figure 7(b). Note that here we cannot easily write the motif of dots directly in the tiles (see figure 7(b)), however, the mapping is still unambiguous.

Let us determine the number of fermions per motif. First of all, in a segment with $f_2 > 0$, the number of fermions is determined by the length of the corresponding S_2 chain. It is easily verified, that for a segment with n empty S_1 sites the corresponding chain has length $2n - 2$. Moreover, from Theorem 5.1, we know that an element in the cohomology of Q on a chain with length $L = 2n - 2$ contains $[(2n - 2)/3]$ fermions, where $[a]$ is the nearest integer to a. Similarly, we find that a segment with k dots contains $[2k/3]$ fermions. Thus a segment with $f_2 = 0$, consisting of k dots and a the pair of bounding sites, contains $[2k/3] + 2$ fermions. From these formulae we find for the four basis motifs "100," "1100," "10000" and "110000," that

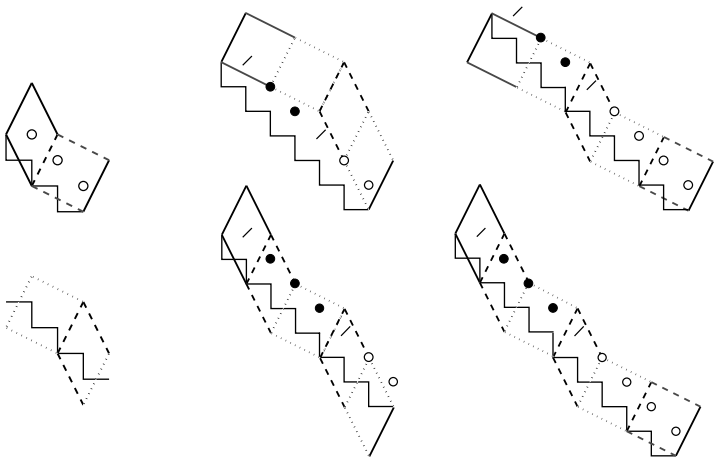

(a) (b)

Figure 7: On the left we show the sequences of tiles that correspond to the motifs with three zeroes (top) and three dots (bottom). The addition of three zeroes to a basis motif corresponds to attaching the sequence of tiles corresponding to the three zeroes to the sequence of tiles corresponding to the basis motif. An insertion of three dots in a basis motif corresponds to inserting the sequence of tiles corresponding to the three dots at the dotted line along the $(1, 2)$ direction in the sequence of tiles corresponding to the basis motif. The insertions of three dots in each of the four basis motifs and the corresponding tiling are shown on the right as examples. From these examples it is clear that we cannot write the three dots directly in the corresponding sequence of tiles. However, the mapping is still unambiguous.

they contain two, three, three and four fermions, respectively. Furthermore, an insertion of three zeroes, corresponds to increasing n by 3, and thus increasing the number of fermions, $[(2n-2)/3]$, by 2. Equivalently, inserting three dots corresponds increasing k by 3, and thus again increasing the number of fermions, $[2k/3]$, by 2. If we compare this to the number of tiles in the tilings that correspond to these motifs, we find that they exactly agree. Furthermore, the number of sites in a motif is given by three times the number of S_1 sites in a motif, since there are two S_2 sites for every S_1 site. On the other hand, for the tiles we find that the area of the diamond is 4 and the area of the square is 5. It is now easily verified that the number of fermions per site for the motifs is the same as the number of tiles per area for the corresponding tiling. Thus we find that, not only is the number of elements in the cohomology of Q directly related to the number of tilings with the two tiles of figure 5(a), but also the number of fermions for each element corresponds to the number of tiles in the corresponding tiling.

One can verify that with these sequences of tiles, and the rules for concatenating them, one can obtain every possible tiling. Each tile can be preceded by a certain type of square and diamond and it can be followed by another type of square and diamond. In total this gives four possibilities for the surrounding neighbors. It can be checked that for each tile all four possibilities can be constructed with the given sequences of tiles and the rules for concatenating them.

Finally, the configurations with all zeroes or all dots account for the extra term in (4.1) in Theorem 4.1 repeated here for convenience:

$$\Delta_i \equiv \begin{cases} -(-1)^{(\theta_m+1)p}\theta_d\theta_{d*} & \text{if } i = [2m/3]p, \\ 0 & \text{otherwise.} \end{cases} \tag{5.7}$$

Remember that

$$\theta_d \equiv \begin{cases} 2 & \text{if } d = 3k \text{ with } k \text{ integer,} \\ -1 & \text{otherwise} \end{cases} \tag{5.8}$$

and with $\vec{v} = (1, 2)$ and $\vec{u} = (m, -m)$ we have $p = 1$, $d = \gcd(u_1 - u_2, v_1 - v_2) = \gcd(2m, -1) = 1$ and $d^* = \gcd(u_1 + u_2, v_1 + v_2) = \gcd(0, 3) = 3$. It follows that the extra term is -2 for $m = 3n$ and $+2$ otherwise.

Let us consider the configuration with all zeroes, which clearly has periodicity 1. If the number of zeroes is a multiple of three, i.e., $m = 3n$, the configuration accounts for two ground states, otherwise it accounts for one ground state. The number of fermions in this configuration is $i = [2m/3]$, i.e. the nearest integer to $2m/3$. From the mapping (figure 7(a)) it is clear that the configuration corresponds to a tiling with periodicity 3 if $m = 3p$. If $m \neq 3p$, however, there is no corresponding tiling. Exactly the same holds for the configuration with all dots. It follows that for $m = 3p$ the tilings overcount the number of ground states by 2 and for $m \neq 3p$ the tilings fail to count 2 ground states.

Note that the choice of sublattices S_1 and S_2 has increased the number of tilings unrelated by a lattice symmetry by a factor of three (see figure 5). Indeed when computing the number of ground states with the motifs given in step 2 it turns out that one discovers each tiling three times (given that the tiling is not completely uniform, that is all diamonds or all squares).

Example 5.4. Let us consider the case of Example 5.3 again. So we have $\vec{v} = (1, 2)$ and $\vec{u} = (10, -10)$. One possibility is to cover the lattice with six squares. This tiling has a unit cell of size 5 and thus this tiling accounts for five ground states. The number of tiles is six and thus the ground states will have six fermions. We can also cover the lattice with two squares and

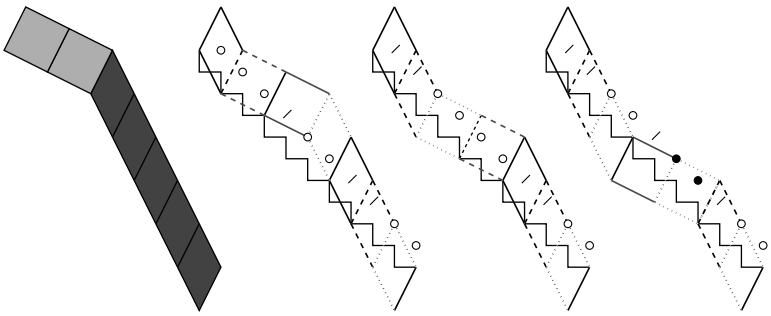

Figure 8: The square lattice with periodicities $\vec{v} = (1, 2)$ and $\vec{u} = (10, -10)$ can be tiled with two squares and five diamonds. One of these tilings, with the two squares adjacent is shown on the left. The choice of sublattices splits this tiling into three tilings. These three tilings and their corresponding motifs are shown on the right.

five diamonds. The two squares can be placed between the diamonds in three independent ways. Each of these three tilings has a unit cell of size 30 and consists of seven tiles, so they account for 90 ground states with seven fermions.

We compare this with the 12 configurations found in example 5.3. The motif "1000010000" has periodicity 5 and accommodates six fermions, so this corresponds to the uniform tiling with all squares. The configurations with all zeroes and all dots account for two ground states with seven fermions and have no corresponding tiling. Finally, there are nine configurations with periodicity 10 and seven fermions, which account for 90 ground states. Using the mapping given in figure 6, we find that these configurations can be split into three groups of three, each group corresponding to one of the tilings with two squares and five diamonds. For example the motifs "1100000100," "1100110000" and "1100 1 · ·100" correspond to the tiling where the two squares are adjacent. They can be distinguished by considering for example the first of the two squares. In each motif it will be of a different type, where the three types are given in figure 5(b) (see figure 8).

5.3.2 The general case: S_2 consisting of p chains

In the previous section we had $\vec{v} = (1, 2)$. In this section we relax this condition to $\vec{v} = (v_1, v_2)$ with $v_1 + v_2 = 3p$ with p a positive integer. It follows that we get p S_2 chains with their accompanying S_1 sites stacked on top of each other. For this situation we will prove Theorem 4.1. The proof consists of five steps:

1. We compute H_{Q_2}.
2. We compute $H_{12} = H_{Q_1}(H_{Q_2})$.

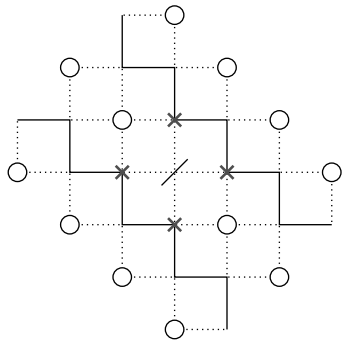

Figure 9: A configuration is shown where an occupied S_1 site is surrounded by empty sites. This sites isolates a site on the S_2 chains directly below and above the site.

3. We compute H_Q starting from H_{12} via the "tic-tac-toe" procedure.
4. We relate the elements of H_Q to tiling configurations by relating each motif to a small series of tiles.
5. We compute Δ_i.

Step 1. As in the previous section we shall start by computing the cohomology of Q_2. We will define two types of configurations that do not belong to H_{Q_2} and then find that H_{Q_2} consists of all configurations except these two types.

Lemma 5.6. *A configuration that contains an occupied site (k,l) on the S_1 lattice, such that the sites $(k+1,l+2)$ and $(k+2,l+1)$ and/or the sites $(k-1,l-2)$ and $(k-2,l-1)$ are empty, does not belong to H_{Q_2}.*

Proof. It is easily verified (see figure 9) that in this configuration the S_2 sublattice contains the isolated site(s) $(k+1,l+1)$ and/or $(k-1,l-1)$. This site can be either occupied or empty, which leads to a vanishing H_{Q_2}. □

Note that in the previous section this situation never occurred because for each occupied site (k,l), the sites $(k+1,l+2)$ and $(k-1,l-2)$ were automatically occupied due to the boundary condition set by $\vec{v}=(1,2)$. The second type of configuration that does not belong to H_{Q_2} follows from a generalization of Lemma 5.2. Remember that occupying S_1 sites causes the S_2 chains to break into smaller open chains. The length of these open chains now depends on the number of empty S_1 sites directly below and above the S_2 chain. For an example see figure 10.

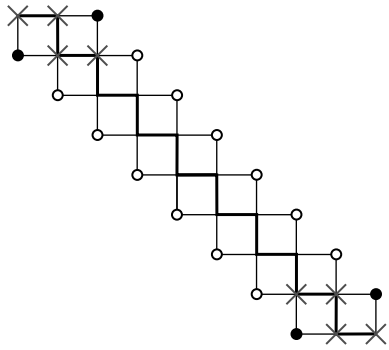

Figure 10: Part of a configuration is shown. The number of empty S_1 sites directly below and above the S_2 chain is 12. The S_2 sublattice thus contains an isolated chain of length 10. Consequently, this configuration does not belong to H_{Q_2}.

Lemma 5.7. *If, for a certain configuration, the sum of the number of empty S_1 sites directly below and above an open S_2 chain is $3s$, the configuration does not belong to H_{Q_2}.*

Proof. It is easily verified that the open S_2 chain corresponding to the $3s$ empty S_1 sites has length $3(s-1)+1$. This leads to a vanishing H_{Q_2}. □

A configuration does not belong to H_{Q_2} if it contains one or more isolated open chains on the sublattice S_2 with length $3p+1$. It is easy to see that all such configurations fall into the class of configurations described in Lemma 5.6, or Lemma 5.7, or both. It follows that all configurations that do not fall into either of these classes belong to H_{Q_2}.

Step 2. As in the previous section, we will now compute $H_{12} = H_{Q_1}(H_{Q_2})$.

Definition 5.3. Define a row of S_1 sites as the set of S_1 sites directly above one S_2 chain.

Note that the configurations in H_{Q_2} again contain segments where f_2, the number of fermions on the S_2 sublattice, is zero and segments where it is non-zero.

Lemma 5.8. *Lemma* 5.4 *for H_{12} holds for each row of S_1 sites.*

That is, in the segments where $f_2 = 0$, the cohomology of Q_1 vanishes when the number of S_1 sites between any pair of bounding sites is $3p+1$ and it contains one element otherwise. The proof can be found in the previous

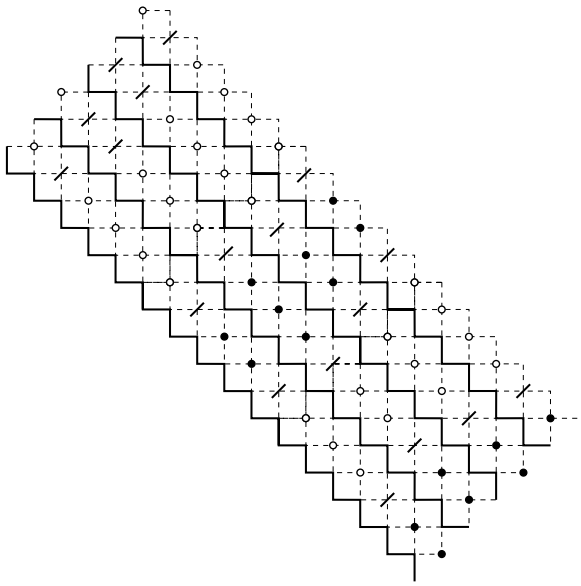

Figure 11: Part of a configuration is shown.

section. It follows that, in the segments where $f_2 = 0$, two types of configurations on a row of S_1 sites are allowed. Using the notation of the previous section, the two types can be distinguished by containing $3s - 1$ dots or $3s$ dots.

Lemma 5.9. *The configurations in H_{12} have spatially separated columnar segments where $f_2 = 0$ and segments where $f_2 > 0$. The width of a column in a segment where $f_2 = 0$ can vary between $3s + 1$ and $3s + 2$ S_1 sites, whereas the width of a column in a segment where $f_2 > 0$ can vary between $3p - 1$ and $3p + 1$ S_1 sites. In the latter case, two consecutive rows never both have width $3p$ and the difference in their widths is at most 1 (or -1).*

Proof. This follows from combining Lemmas 5.6–5.8. □

An example is shown in figure 11. From Lemma 5.9 it follows that we only have to consider columns of width varying between 1 and 2 in the segments where $f_2 = 0$ separated by columns of width varying between 2 and 4 in the segments where $f_2 > 0$. All other configurations can be obtained from these configurations by inserting multiples of three dots in the segments where $f_2 = 0$ over the entire height of the columns, and, similarly, by inserting multiples of three zeroes in the segments where $f_2 > 0$ over the entire height of the columns.

We now turn to the segments where $f_2 > 0$. Remember that in the previous section this step was easy because all S_1 sites in the segment where $f_2 > 0$ were blocked by fermions on the S_2 chain. Here, however, that is not the case. The first thing we note in this case is the following.

Lemma 5.10. *The S_1 sites within a column marking a segment where $f_2 > 0$ have to be empty if they are away from the boundaries with adjacent columns marking a segment where $f_2 = 0$.*

Proof. This follows directly from Lemma 5.6. □

From this lemma it follows that we only have to consider the S_1 sites on the boundary between a segment where $f_2 > 0$ and a segment where $f_2 = 0$. In fact, we will argue that we only have to consider the boundary where the segment with $f_2 > 0$ is to the right of a segment with $f_2 = 0$ (and not the boundary on the other side).

First, however, we introduce a new notation where a configuration is fully characterized by the boundaries between the two types of segments ($f_2 = 0$ and $f_2 > 0$). From Lemma 5.6 it follows that these boundaries are an arbitrary sequence of steps of $+(2,1)$ and $+(1,2)$. However, in the new notation we shall tilt the lattice by $-45°$, such that the rows of S_1 sites are horizontal. If we then draw the boundary as a collection of vertical lines between two S_1 sites that are to the left and to the right of the boundary, we find that the boundaries have a zigzagged shape. The segments where $f_2 > 0$ will be white and the segments where $f_2 = 0$ will be gray. For an example see figure 12.

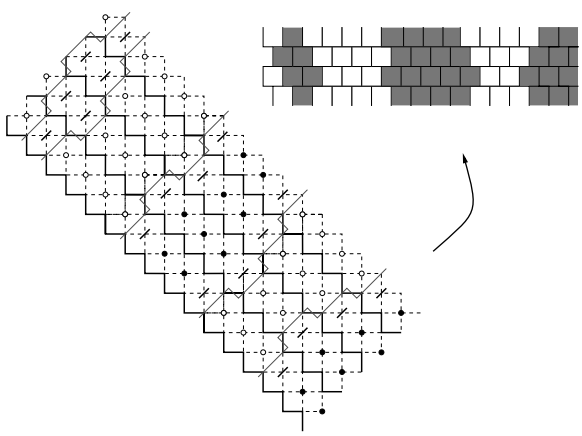

Figure 12: Part of a configuration is shown with a mapping to the new notation.

Suppose for a moment that we would have a completely disconnected graph, that is, just a collection of disconnected vertices. Then each site can be both empty and occupied. It is clear that each configuration with a least one empty site does not belong to the kernel of Q, whereas each configuration with at least one occupied site belongs to the image of Q. It follows that H_Q vanishes at all grades. Here we do not have a disconnected graph, however, it turns out that the division in gray and white regions is similar to disconnecting the graph.

We define a special notation for a site that can be both empty and occupied. If this site is to the right of a gray region we shall denote this site with a dot, whereas when it is to the left of a gray region the site will be shaded. That is, suppose there are two configurations that both belong to H_{Q_2} and obey Lemma 5.9, such that these two configurations differ by one site only. Then we can summarize these two configurations in one picture by denoting this particular site by a dot if it is to the right of a gray region or by shading the site if it is to the left of a gray region. For an example see figure 13. Moreover, we can summarize 2^n configurations in one picture if the picture contains n sites with dots or shaded sites. We make a distinction between sites to the left and to the right of the grey region, because we will argue that the configurations with a site with a dot do not belong to H_{12}. Clearly this is a choice, we could also have chosen to argue that the configurations with a shaded site do not belong to H_{12}.

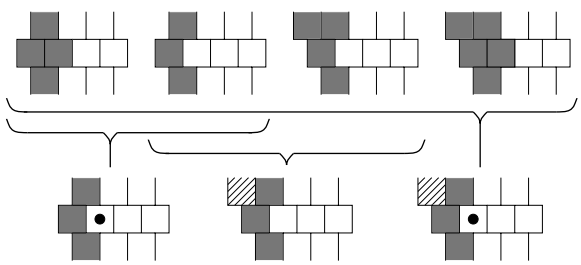

Figure 13: The big brackets indicate how the configurations at the top can be summarized using the notation introduced in the text. The two left-most configurations at the top differ by one site in the *right*-most boundary of the gray region, they can therefore be summarized by the left-most picture at the bottom by denoting this site with a dot. The middle two configurations at the top differ by one site in the *left*-most boundary of the gray region, they can therefore be summarized by the middle picture at the bottom by shading this site. Finally, all four configurations at the top can be summarized by the right-most picture at the bottom.

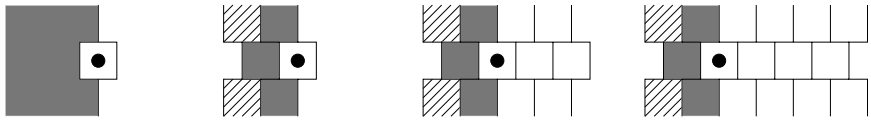

(a) (b) (c)

Figure 14: In three steps we find that there are eight possible configurations with a site with a dot in a boundary that separates a gray segment on the left from a white segment on the right: (a) It follows from Lemma 5.6 that a site with a dot must have occupied sites to the upper left and lower left and empty sites to the upper right and lower right. (b) There are four possibilities for the left-most boundary of the gray segment, following from the two shaded sites being empty or occupied. (c) There are two possibilities for the right-most boundary of the white segment.

Let us consider a boundary that separates a grey segment on the left from a white segment on the right. There are only a few such configurations that may have a site on the boundary with a dot.

Lemma 5.11. *There are eight possible configurations with a site with a dot in a boundary that separates a gray segment on the left from a white segment on the right. The configurations are depicted in figure* 14*(c).*

Proof. The first restriction follows from Lemma 5.6. That is, both when the site is empty as well as when it is occupied, the configuration should satisfy the lemma. This restriction is depicted in figure 14(a). Then the second restriction follows from Lemma 5.8, that is, the width of a grey column varies between 1 and 2 modulo 3. It follows that next to the site with the dot there can only be one gray site (modulo 3). Combining this again with Lemma 5.6, we find four possibilities for the left boundary of the gray segment. The four possibilities can be summarized in one picture with the notation defined above, see figure 14(b), the shaded sites can be both empty and occupied. Finally, it follows from Lemma 5.7 that there are only two possible right-most boundaries for the white segment, each modulo columns of width 3, see figure 14(c). □

From Lemma 5.11 it follows that if there is more than one site with a dot in the same boundary, they are sufficiently far away to be independent. That is, each of these sites can be both empty and occupied independent of the configuration of the other dotted sites. Also note that if we select one of the eight configurations with a dot from figure 14(c), the rest of the system can take on any configuration independent of the configuration of the dotted site. Note that this resembles a disconnected graph.

We are now ready to solve $H_{Q_1}(H_{Q_2})$.

Lemma 5.12. *All configurations that contain a boundary between a gray segment to the left and a white segment to the right, such that this boundary contains one or more sites with a dot, do not belong to* $H_{Q_1}(H_{Q_2})$.

Proof. A site with a dot can be either empty or occupied. Suppose the site is empty and we act with Q_1 on the configuration. If Q_1 can act non-trivially only on the site under consideration we are done, since the configuration in which the site with the dot is empty does not belong to the kernel of Q_1 and the configuration in which it is occupied belongs to the image of Q_1. This proves the lemma for this case.

If, however, Q_1 can act non-trivially also on other sites, there are four scenarios: (a) The other site is in the same boundary. (b) The other site is in the left boundary of the gray region under consideration. (c) The other site is in the right boundary of the white region under consideration. (d) The other site is further away from the region under consideration than the first three cases.

For scenario (a), we know that the other site is also a site with a dot. It follows that the configuration with both dotted sites empty does not belong to the kernel of Q_1. The sum of the configurations with one of the dotted sites empty belongs to the image of Q_1. The difference of the configurations with one of the dotted sites empty does not belong to the kernel of Q_1, because it maps to the configuration with both dotted sites occupied. Clearly, the latter configuration belongs to the image of Q_1. So for this scenario the lemma is proven.

For scenario (b) we distinguish two cases. First, the other site and the dotted site can be occupied simultaneously. In this case we can prove the lemma via the same argument as we did for scenario (a). Second, the other site and the dotted site *cannot* be occupied simultaneously. This only happens when the other site is in the same row as the dotted site. In this case the sum of the configurations with one of them occupied is in the image of Q_1, but the difference belongs to the kernel of Q_1 and does not belong to the image of Q_1. The latter is thus an element of $H_{Q_1}(H_{Q_2})$. However, we have the freedom to decide to keep only the configuration in which the other site is occupied and the dotted site is empty as a representative of this element. At this point it becomes clear why we only consider configurations with a site with a dot, and not configurations with a shaded site.

For scenario (c) we can again distinguish two cases. In the first case, the configuration of the other site and the dotted site are independent and

the lemma is proven as for scenario (a). In the second case, the other site and the dotted site *cannot* be occupied simultaneously. There are again three configurations under consideration. The configuration with both sites empty does not belong to $\ker Q_1$, the sum of the configurations with one of the two sites occupied belongs to $\operatorname{Im} Q_1$ and, finally, the difference again is an element of $H_{Q_1}(H_{Q_2})$. And as under (b), we choose to represent this element with the configuration where the dotted site is empty and the other site occupied.

Finally, for scenario (d) it is clear that the configuration of the other site and the dotted site are always independent and the lemma is proven as for scenario (a).

In the four scenarios we considered, there was just one other site on which Q_1 acts non-trivially. If there are more sites on which Q_1 acts non-trivially, the lemma clearly holds when these sites can again be empty or occupied independent of the dotted site. However, if they are not all independent, the proof is more lengthy, but analogous to the proofs of the second case in scenarios (b) and (c).

□

Lemma 5.13. *All the configurations that belong to $H_{Q_1}(H_{Q_2})$ are a sequence of alternating gray and white columns subject to the conditions in Lemma* 5.9*, such that the left-most boundary of all the white columns does not contain any sites with a dot.*

Proof. This is a direct consequence of Lemma 5.12. □

As an example we consider the case where $\vec{v} = (6, 6)$ and $\vec{u} = (m, -m)$, that is, we stack four rows of m S_1 sites separated by four S_2 chains. All configurations in H_{12} can be obtained by concatenating the configurations depicted in figure 15, with eventual insertions of grey and/or white columns of width 3, such that the boundary conditions are satisfied.[3] That is, each row should in the end have width m or, equivalently, the right-most boundary should fit with the left-most boundary. Finally, there is a configuration with all zeroes (one entirely white segment) and a configuration with all dots (one entirely grey segment).

Step 3. In the previous step we have determined H_{12}. According to the "tic-tac-toe" lemma, the cohomology of Q is equal to or contained in H_{12}:

[3]These configurations are obtained as follows. First consider all possible white segments satisfying the boundary condition in the $\vec{v}$-direction, then construct all possibilities for the gray segments to the left of these white segments.

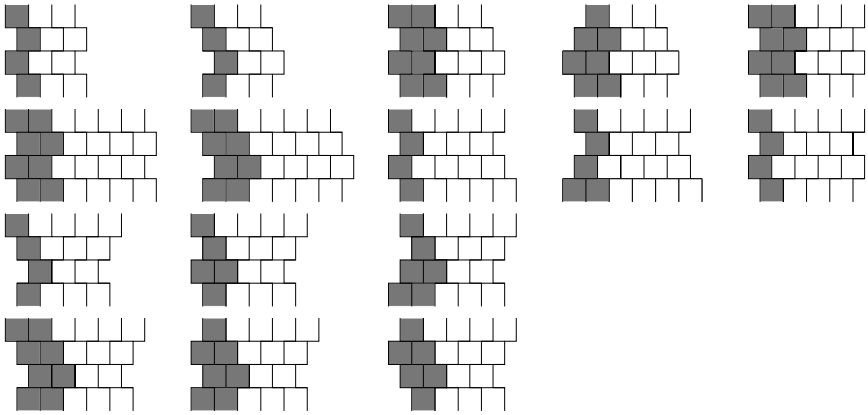

Figure 15: Building blocks of the configurations spanning $H_{Q_1}(H_{Q_2})$ for $\vec{v} = (6, 6)$ and $\vec{u} = (m, -m)$, modulo insertions of grey and white columns of width 3.

$H_Q \subseteq H_{12}$. In the previous section we found that for $\vec{v} = (1, 2)$, we have $H_Q = H_{12}$. For general $\vec{v}$, however, this is not the case. That is, within H_{12}, there are configurations that are not in the kernel of Q and there are configurations that are in the image of Q. To find out which configurations do not belong to H_Q, we follow the "tic-tac-toe" procedure [16] as described in step 3 of Section 5.3.1.

In the previous section, we found via the "tic-tac-toe" procedure that we could find for each element $|\psi_0\rangle$, that belongs to H_{12}, but not to $\ker Q$, an element $|\psi_n\rangle$ that does belong to $\ker Q$. In this section, however, we will find that for some elements $|\psi_0\rangle$, the "tic-tac-toe" procedure leads to a corresponding element $|\tilde{\psi}\rangle$, that also belongs to H_{12}. We then say that $|\psi_0\rangle$ maps to $|\tilde{\psi}\rangle$ at the end of the "tic-tac-toe" procedure and we conclude that neither $|\psi_0\rangle$ nor $|\tilde{\psi}\rangle$ belong to H_Q.

We now prove some rules for the "tic-tac-toe" procedure specific to the configurations we obtained in the previous step.

Lemma 5.14. *Let Q act on an empty S_1 site (k, l), such that for the preceding S_1 sites on that row we have: $(k-1, l+1)$ and $(k-3s-2, l+3s+2)$ are occupied and the intermediate sites are dotted. Then the new configuration with (k, l) occupied, is also the image of Q_1 acting on the configuration with (k, l) occupied and one less fermion in the preceding sites $(k-1, l+1)$ to $(k-3s-1, l+3s+1)$.*

Proof. For general s we can denote the original configuration as "$1 \cdot_{3s} 10$," the new configuration is then "$1 \cdot_{3s} 11$." From Lemma 5.4 we know that,

if the number of S_1 sites between a bounding pair is $3s+1$, H_{Q_1} vanishes. Consequently, each configuration that is in the kernel of Q_1 is also in the image of Q_1. Now, since the configuration "$1 \cdot_{3s} 11$" is in the kernel of Q_1 and the number of S_1 sites between the bounding pair is $3s+1$, it must also be in the image of Q_1. Thus, there is a configuration with one less fermion between the bounding pair that maps to this configuration under the action of Q_1. □

Example 5.5. For $s=0$ this is easily understood: the original configuration will have "110" on the S_1 sites $(k-2, l+2)$ through (k,l). Acting on this with Q gives "111," however, this can also be obtained by acting with Q on $-$"101."

Lemma 5.15. *Acting with Q on a white segment away from the boundary, gives zero.*

Proof. The proof is analogous to the proof of Lemma 5.3. The length of the S_2 chains in the white region is $L=3k$ or $L=3k-1$ each containing k fermions. If Q_1 acts on a site above this chain and away from the boundary, it will cut the S_2 chain into three pieces. One of length 1 and two of lengths L_1' and L_2', such that $L_1'+L_2'=L-3$. We will now argue that the new configuration with the smaller S_2 chains, always belongs to $\operatorname{Im} Q_2$. This implies that we can always continue to the next step in the "tic-tac-toe" procedure.

If the chain of length 1 contains a fermion, the new configuration clearly belongs to $\operatorname{Im} Q_2$. If it is empty there are k fermions on the other two chains. For $L=3k$ their combined length is $L_1'+L_2'=3(k-1)$, so $L_1'=3k_1$ and $L_2'=3k_2$ or $L_1'=3k_1+1$ and $L_2'=3k_2-1$, where in both cases $k_1+k_2=k-1$. For the second case the cohomology vanishes for all fermion numbers because of the length L_1'. For the first case the cohomology is non-vanishing only if $f=k_1+k_2=k-1$, however, there are k fermions. So for both cases the new configuration belongs to $\operatorname{Im} Q_2$ (since it belongs to $\ker Q_2$ and not to H_{Q_2}). For $L=3k-1$ we find $L_1'=3k_1$ and $L_2'=3k_2-1$ or $L_1'=3k_1+1$ and $L_2'=3k_2-2$, where in both cases $k_1+k_2=k-1$. The rest of the argument is the same as before.

From the above it follows that we can always continue with the next step in the "tic-tac-toe" procedure. Now suppose that in this next step we act with Q_1 on the same row as in the first step. Since there are no fermions between these two S_1 sites, this configuration will cancel against the configuration where the two S_1 sites are occupied in the reverse order. It follows that we only have to consider acting with Q_1 on each row just once.

It is now easily verified that, since there are as many S_2 chains as there are S_1 rows, we can always continue the "tic-tac-toe" procedure until we get zero. □

In this lemma we restricted ourselves to Q acting on S_1 sites away from the boundary. We will see in the following that if we allow Q to act on sites at the boundary, the "tic-tac-toe" procedure can map one configuration in H_{12} to another configuration in H_{12}. The crucial point is that, when we act with Q_1 on a site at the boundary, the length of at least one of the S_2 chains below and above this site is reduced by 1. If the original length was $3k$, the new length is $3k-1$ and both have non-vanishing cohomology for $f=k$. In that case we cannot use this S_2 chain to write the new configuration as Q_2 of some other configuration. It follows that to continue the "tic-tac-toe" procedure, we have to use the other S_2 chain. However, if this chain was already used in a previous step, the "tic-tac-toe" procedure could end. Before we continue with an example that illustrates this point, we will argue that it is enough to consider Q acting only on sites at the boundary. This follows from Lemma 5.9; if the "tic-tac-toe" procedure ends because we have obtained a configuration that does not belong to $\operatorname{Im} Q_2$ (nor to $\operatorname{Im} Q_1$), this configuration must belong to H_{12}. From Lemma 5.9 we know that configurations in H_{12} have spatially separated columnar gray and white segments that do not branch. It follows that we can only map one configuration in H_{12} to another by either creating a new gray column in a white column, or by (locally) increasing the width of a gray column. Since the first possibility is excluded by Lemma 5.15, we conclude that we can restrict Q to act only on sites at the boundary. As in step 2 we will restrict ourselves to the left-most boundary to avoid overcounting.

Let us consider an example of a configuration that does belong to H_{12}, but does not belong to H_Q, i.e., it maps to another configuration in H_{12} at the end of the "tic-tac-toe" procedure.

Example 5.6. Consider the configuration shown on the left in figure 16. We label the three S_2 chains (not shown explicitly) between the four S_1 rows; chain 1, chain 2 and chain 3 (c_1, c_2 and c_3) from top to bottom. Similarly, we label the S_1 rows; row 1 to row 4 (r_1 to r_4) from top to bottom. The S_2 chains have lengths $L_{c_1}=6$, $L_{c_2}=5$ and $L_{c_3}=3$ and thus contain 2, 2 and 1 particle, respectively. Now consider the left-most, empty S_1 sites in the middle two rows. Occupying the left-most, empty S_1 site on row 2 reduces the length of c_1 from 6 to 5. There will still be two particles on c_1 and since the chain of length 5 has non-vanishing cohomology at grade 2, the configuration on this chain will in general not belong to $\operatorname{Im} Q_2$. Occupying the left-most, empty S_1 site on row 3 reduces the length of c_3 from 3 to 2.

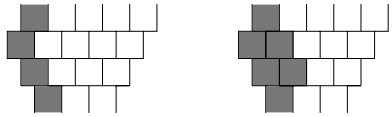

Figure 16: On the left we depict the configuration that does belong to H_{12}, but not to H_Q, since it does not belong to the kernel of Q. Instead it maps to the configuration depicted on the right under the "tic-tac-toe" procedure. This configuration also belongs to H_{12}, but not to H_Q, since it belongs to $\operatorname{Im} Q$. The configuration on the left has four particles on sublattice S_1 and five particles on sublattice S_2, divided as 2, 2, 1 over the S_2 chains from top to bottom. The configuration on the right has one more particle in total; it has six particles on S_1 and it has four particles on S_2, divided as 2, 1, 1 over the S_2 chains from top to bottom.

Again the configuration on this chain will not belong to $\operatorname{Im} Q_2$, since the chain of length 2 has non-vanishing cohomology at grade 1. It follows that if we occupy either of these S_1 sites in the "tic-tac-toe" procedure, we have to use c_2 to write the new configuration as Q_2 of some other configuration. By definition this is always possible in the first step of the procedure. However, also by definition, we can do this only once since $Q^2 = 0$. It follows that, after two steps in the "tic-tac-toe" procedure, we obtain a new configuration (see figure 16 on the right) that has 2, 1 and 1 particles on the S_2 chains from top to bottom and belongs to H_{12}. Consequently, both the original as well as the final configuration do not belong to the cohomology of Q, although they do belong to H_{12}.

As we anticipated, the crucial point in this example is that the length of an S_2 chain is reduced from $3k$ to $3k-1$, since this limits the options to continue the "tic-tac-toe" procedure. In fact, in the "tic-tac-toe" procedure, we can only reach a configuration that is not in the image of Q_2 if the length of an S_2 chain is reduced from $3k$ to $3k-1$. To find the configurations in H_{12} that map to another configuration in H_{12} under the action of Q in the most efficient way,[4] we will start the "tic-tac-toe" procedure by occupying an S_1 site, such that this happens. It follows that we can then only use the other S_2 chain to continue the procedure. We will then, again for efficiency, continue the procedure by again occupying an S_1 site such that there is just one S_2 chain that we can use to continue the procedure. This means that we

[4]By "the most efficient way" we mean the shortest sequence of occupying S_1 sites in the "tic-tac-toe" procedure that maps one configuration in H_{12} to another. This is the most efficient way, because as soon as this happens, we know that both configurations do not belong to H_Q, independent of all the other terms created under the action of Q.

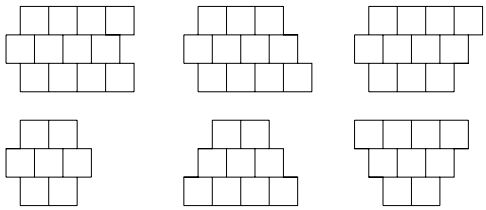

Figure 17: The possible boundaries of a white segment are shown, such that the left-most boundary contains a critical reducer site. That is, occupying this site reduces the length of at least one of the adjacent S_2 chains from $3k$ to $3k-1$.

will act with Q_1 on consecutive rows, either moving upwards or downwards along the boundary.

In the previous step we constructed all possible configurations with a site *with a dot* in the left-most boundary of a white segment. Here we will construct all possible configurations with a site in the left-most boundary of a white segment, such that occupying this site reduces the length of an S_2 chain from $3k$ to $3k-1$. We shall call such sites "critical reducer sites." We start with the white segment and obtain the configurations depicted in figure 17. For these configurations occupying the left-most site of the middle row reduces the length of at least one of the adjacent S_2 chains from $3k$ to $3k-1$. For the two configurations on the left, occupying this site reduces the length of both S_2 chains to $3k-1$. It follows that the new configuration must belong to $\operatorname{Im} Q_1$ (see Lemma 5.14), otherwise it was a site with a dot in the previous step. So we do not have to consider these two configurations. This same reasoning tells us that the gray region to the left of the middle row should have width 1 modulo 3, otherwise the new configuration would belong to $\operatorname{Im} Q_1$. This leads to the 12 possibilities in figure 18.

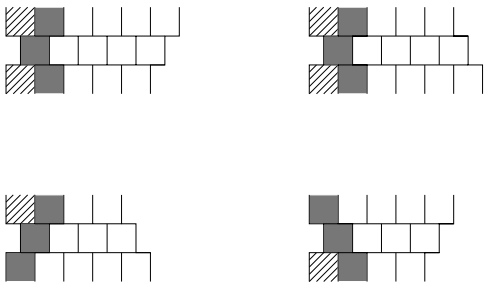

Figure 18: The 12 possible configurations such that the left-most site of the middle row is a critical reducer and occupying this site does not lead to a configuration that is in $\operatorname{Im} Q_1$.

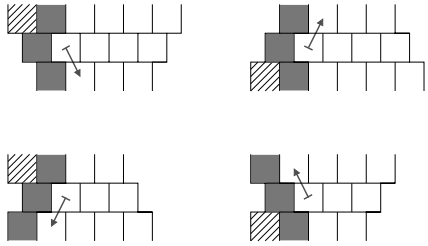

Figure 19: If the critical reducer site (the left-most site of the middle row) is occupied in the first step of the "tic-tac-toe" procedure, the procedure should be continued in one direction only, as explained in the text. This direction is indicated by the arrow.

Note that, indeed, occupying the critical reducer site at the boundary, leads to reducing the length of one of the S_2 chains from $3k$ to $3k-1$, for all these configurations. For efficiency we continue the "tic-tac-toe" procedure either upwards or downwards, such that at every step in the procedure there is just one S_2 chain that we can use to continue the procedure. The direction we should follow, is indicated by the arrow in figure 19. Note that we dropped the two configurations for which the grey segment had width 2, because of Lemma 5.14.

It is now clear that if we stack a configuration for which the "tic-tac-toe" procedure goes downwards on top of a configuration for which it goes upwards, the "tic-tac-toe" procedure ends. In particular, it maps the old configuration to a new configuration that is also in H_{12}. We can increase the number of steps necessary in the "tic-tac-toe" procedure by stacking rows for which the grey segment has width 1 modulo 3 and the width of the white segment alternates between 3 and 4 modulo 3 (see figure 20). Examples of the stacked configurations and the configurations they map to are shown in figure 21. Here the sites with connected dots can be either all empty or all occupied. The configuration with all the sites empty maps to the configuration with all the sites occupied under the "tic-tac-toe" procedure. However, if the configurations on the left in figure 19 are not combined with one of the configurations on the right in figure 19, the "tic-tac-toe"

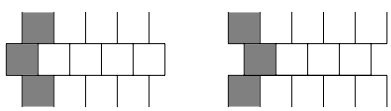

Figure 20: Stacking these configurations with the configurations of figure 19, increases the number of steps in the "tic-tac-toe" procedure.

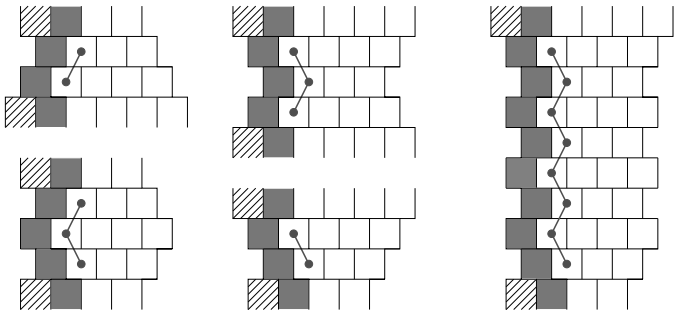

Figure 21: Some examples are shown of configurations that do belong to H_{12}, but not belong to H_Q. Here the sites with connected dots can be either all empty or all occupied.

procedure will end with a state that is in the kernel of Q (as long as we only let the sites on the left-most boundary participate).

At this point we have identified a certain set of configurations that does belong to H_{12}, but does not belong to H_Q. However, we have to make a final step before we can identify all configurations in H_Q with tiling configurations. This is due to the fact that certain parts of configurations seem to belong to H_Q, but they do not respect the boundary conditions. Note that, at this point, we have reduced all possible motifs to the following set:
"100"
"1100"
"10000"
"110000"
which can be separated by single insertions of the motifs:
"1000"
"11000"
all modulo insertions of three dots and three zeroes along an entire column. Each of the four basis motifs, comes with two directions, determined by whether the boundaries between the gray and white segments follows the direction $(-1,-2)$ or $(-2,-1)$.

Definition 5.4. We assign a letter to each of the four basis motifs:

$A_i \equiv$ "100"

$B_i \equiv$ "1100"

$C_i \equiv$ "10000"

$D_i \equiv$ "110000"

where the subscript i is 1 or 2 when the direction of the motif is $(-1,-2)$ or $(-2,-1)$, respectively.

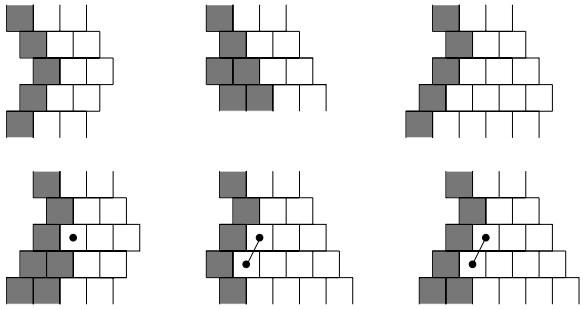

Figure 22: At the top, we show, from left to right, motif A_1 followed by the motifs A_2, B_1 and C_2. On the bottom-left, we see that a configuration in which A_1 is followed by B_2 contains a site with a dot in the left-most boundary of the white segment. The other two configurations on the bottom, show that configurations in which A_1 followed by C_1 or D_i do not belong to H_Q. Here we used the notation of figure 21.

Note that the direction of a motif is not defined if neither the motif directly above it nor the motif directly below it is the same. We will start, however, by considering cases in which this does not happen. At the end of step 4 we will encounter a case where this point needs some attention.

We now want to study whether a vertical sequence of a certain motif can be followed by a sequence of a different motif, eventually, with a insertion of one of the motifs with three zeroes: "1000" or "11000."

Example 5.7. As an example let us start with a sequence of motif A_1. This sequence could be followed by motifs A_2, B_1 and C_2. However, it cannot be followed by motif B_2, because it would not belong to H_{12}. Nor can it be followed by motifs C_1 or D_i, because it would not belong to H_Q (see figure 22).

Similarly we find the following:

- motif B_1 can only be followed by motif C_2;
- motif C_2 can only be followed by motif B_1;
- motif A_i can be followed by motifs A_j, B_1 and C_2;
- motif D_i can be followed by motifs D_j, B_1 and C_2;
- motif B_2 can only follow after motif C_1;
- motif C_1 can only follow after motif B_2.

Finally, we know from Lemmas 5.7 and 5.8 that gray and white columns cannot branch or have end points, since their width always oscillates between 1 and 2 modulo 3 or 2, 3 and 4 modulo 3 for the gray and white segments,

respectively. Consequently, gray and white columns may wind around the torus several times, but they will always close to form a loop.

Let us combine this observation with the rules we found for stacking motifs. Consider, for example, motif A_1, which can be followed by motifs A_2, B_1 and C_2. However, motifs B_1 and C_2 can only be followed by C_2 and B_1, respectively. Consequently, if motif A_1 is followed by either of these two motifs, we can never fulfill the boundary conditions, because the column cannot be closed to form a loop. Thus configurations in which motif A_1 is followed by motifs B_1 and C_2 do not belong to H_Q. In this same spirit we obtain the following lemma.

Lemma 5.16. *For configurations that belong to H_Q the following holds:*

- *motif B_1 can only be followed by motif C_2 and vice versa;*
- *motif A_1 can only be followed by motif A_2 and vice versa;*
- *motif D_1 can only be followed by motif D_2 and vice versa;*
- *motif B_2 can only be followed by motif C_1 and vice versa.*

For motifs A_i and D_i the width of the white segment does not change, thus the motif with direction 1 can follow directly below or above this same motif with direction 2. For the motifs B_i and C_i, however, there is an intermediate motif of the type "1000" or "11000." Which of the two can be determined via the "tic-tac-toe" procedure. If we read the motifs of the rows from top to bottom, we find that a sequence of B_1 motifs will be followed by "1000," to be followed by a sequence of C_2 motifs. Then the C_2 motifs will be followed by "11000," which is then to be followed by another sequence of B_1 motifs. On the other hand, a sequence of B_2 motifs will be followed by "11000," followed directly by a sequence of C_1 motifs. Finally, the C_1 motifs will be followed by "1000," followed directly by another sequence of B_2 motifs (see figure 23). It is readily checked that any other choice gives a configuration that does belong to H_{12}, but not to H_Q.

Step 4. We are now ready to make the identification with the tiles. For the four basis motifs A_1 through D_1 the identification is shown in figure 24 and A_2 through D_2 are identified with a tiling in figure 25. Note that to distinguish motif X_1 from X_2, where $X = A, B, C$ or D, one has to consider also the motif on the row above or below this motif. These motifs can be followed by an arbitrary threefold of zeroes. Let us define the motif $E \equiv$ "000." For this motif we can also distinguish a direction, because its boundary will follow the left-most boundary of the white segment it is attached to. From figures 24 and 25 it is clear that the motifs X_i can be followed by motif E_i,

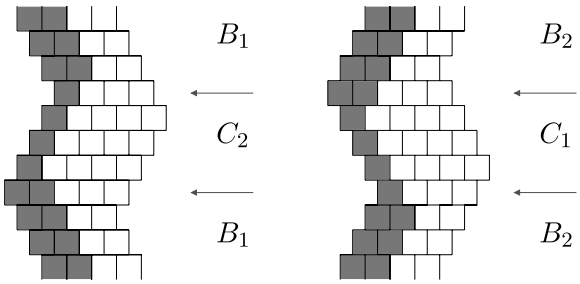

Figure 23: Two configurations are shown in which motif B_i is followed by motif C_j (where $i \neq j$) and vice versa, with the correct intermissions of the motifs "1000" and "11000" (indicated by the arrows).

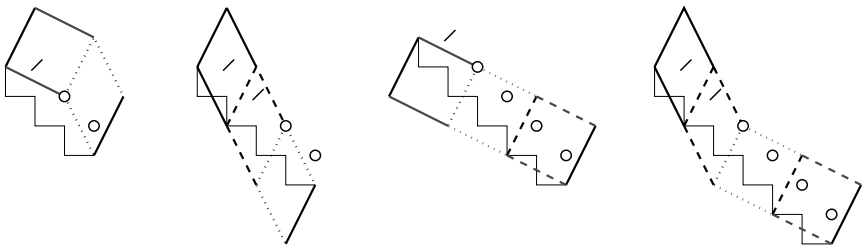

Figure 24: The motifs X_1 and the corresponding tilings. Note that this mapping was already found in Section 5.3.1 (see figure 6).

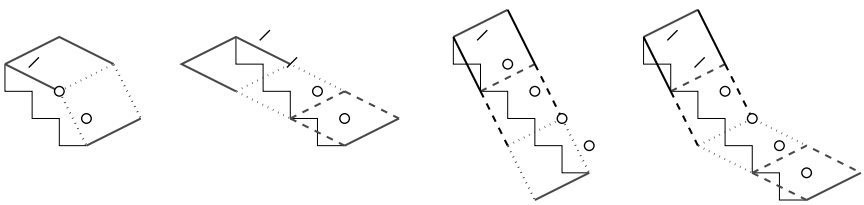

Figure 25: The motifs X_2 and the corresponding tilings.

where the i should be the same. For the motifs B_1 and C_2 there is an exception: when the motif above these motifs is "11000" and "1000," respectively, they are followed by E_2 and E_1, respectively.

There can also be insertions of multiples of three dots in the four basis motifs. How this translates into tilings is shown in figure 26. More precisely, note that each basis motif X_1 contains a dotted line, connecting two S_1 sites along the direction 1 (black) and equivalently, all basis motifs X_2 contain a dotted line with direction 2 (blue). An insertion of three dots in a basis motif corresponds to an insertion of two tiles, shown in figure 27, at this

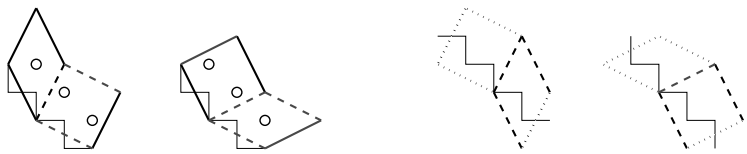

Figure 26: On the left the motifs E_1 (on the left) and E_2 (on the right) and the corresponding tilings. On the right the tilings corresponding to insertions of three dots into the motifs X_1 (on the left) and X_2 (on the right).

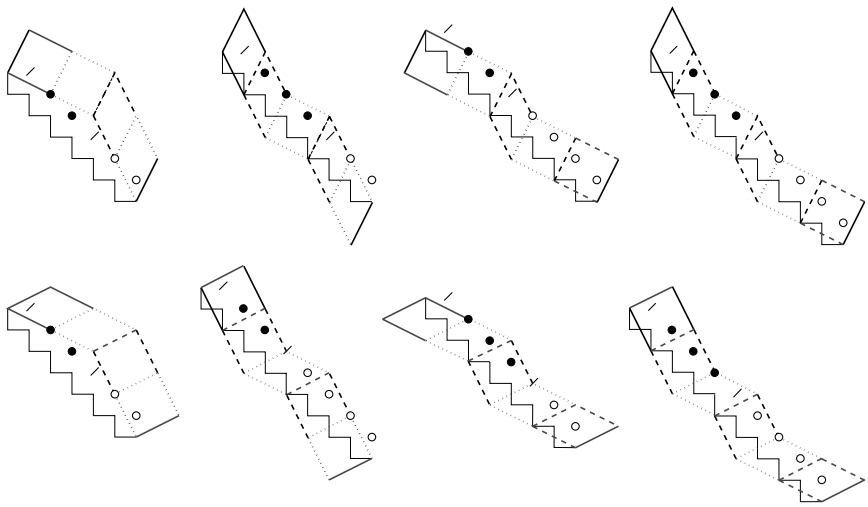

Figure 27: On the top (bottom), insertions of three dots into the motifs X_1 (X_2) and the corresponding tilings are shown.

dotted line. Note that here we cannot easily write the motif of dots directly in the tiles, however, the mapping is still unambiguous.

Finally, we have the motifs "1000" and "11000." Which tilings these motifs correspond to depends on whether they occur between the motifs B_1 and C_2 or the motifs B_2 and C_1. In fact, in the first case, "1000" will correspond to the same sequence of tiles as B_1 and "11000" to the same tiling as C_2. Similarly, in the latter case, "1000" and B_2, on the one hand, and "11000" and C_1, on the other hand, correspond to the same tilings. For an example see figure 28.

With these identifications there is one ambiguity, but it is easily dealt with. If there is a column in which the motifs alternate indefinitely between "1100" and "11000," we cannot determine whether the motif "1100" is of

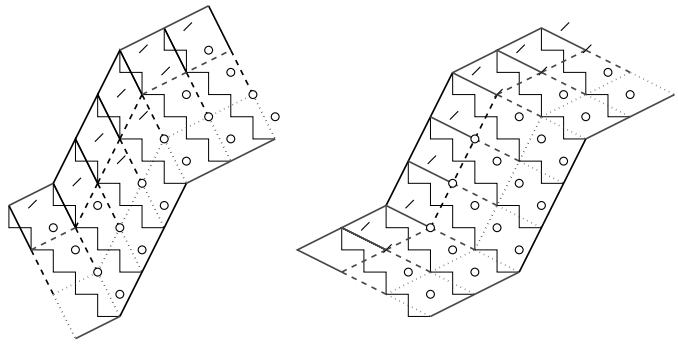

Figure 28: On the left (right), we show a configuration in which motifs C_2 and B_1 (C_1 and B_2) alternate with the corresponding tilings. Note that the motifs "1000" and "11000" correspond to different tilings on the left than on the right.

type B_1 or B_2. The same happens when the motifs "10000" and "1000" alternate indefinitely: the motif "10000" could be of type C_1 or C_2. Note that if we choose to identify the first with B_1 and the second with C_2, the corresponding tilings would be indistinguishable. This also happens when we choose B_2 and C_1. So we conclude that we should either choose B_1 and C_1 or B_2 and C_2. The ambiguity is thus lifted by simply deciding that we will always choose, say, B_1 and C_1.

Finally, we note that again the number of fermions in a certain configuration is the same as the number of tiles in the corresponding tiling. For the four basis motifs and the motifs with three zeroes or three dots, this follows from the arguments in Section 5.3.1. For the motifs "1000" and "11000," we should look at figure 28. If the motif "1000" sits between motifs B_1 and C_2, the number of fermions in these three rows is $3 * 3$ and the number of sites is three times the number of S_1 sites: $3 * (2 * 4 + 5)$. So nine fermions on 39 sites. Compare this with the corresponding tiling: it contains two times three tiles of area 4 and once three tiles of area 5. So nine tiles with total area 39. Similarly, if the motif "11000" sits between motifs B_1 and C_2, the number of fermions in these three rows is $3 * 3$ and the number of sites is $3 * (2 * 5 + 4)$. The corresponding tiling contains two times 3 tiles of area 5 and once three tiles of area 4. For the corners between motifs B_2 and C_1 the comparison is slightly more subtle. Following the same arguments as above, we find that in this case the number of fermions in the motifs "1000" and "11000" do not agree with the number tiles in the corresponding tiling. However, the discrepancy is minus one in one case and plus on in the other, and since the boundary conditions dictate that the number

of "1000"-motifs equals the number of "11000"-motifs, the discrepancies exactly cancel.

Step 5. The final step concerns the small correction Δ in equation (4.1). With the four basis motifs, horizontal insertions of multiples of three dots and three zeroes and vertical insertions of the motifs "1000" and "11000," we can represent all elements in H_Q. With the mappings given in the previous step, we find a corresponding tiling for each of these elements. On the other hand, each possible tiling can be constructed with the small sequences of tiles given in the previous step. Thus we find that for each possible tiling there is a corresponding element in H_Q. Furthermore, we found that the number of fermions and the number of tiles agree. So we find $N_i = t_i$, that is, the number of elements in H_Q with i fermions equals the number of tilings of the square lattice with i tiles. However, there is a small discrepancy in this one-to-one relation for the configurations with all zeroes or all dots. For $\vec{u} = (m, -m)$ and $v_1 + v_2 = 3p$, it is readily verified that these configurations contain $i = [2m/3]p$ fermions. In the following we will first compute the number of elements of H_Q that these configurations account for. We shall call this $N^{(a)}$, where a stands for anomalous. We will then compute $t^{(a)}$, the number of tilings consisting only of the tiles that correspond to either all zeroes or all dots (see figure 26). Combining these results we obtain $\Delta \equiv N^{(a)} - t^{(a)}$. Finally, since we found a one-to-one correspondence between tilings and elements of H_Q for $i \neq [2m/3]p$, Theorem 4.1 will then be established with Δ_i as in equation (4.2).

As we discussed in Section 5.3.1 for $\vec{v} = (1, 2)$, the configurations with all dots and all zeroes actually correspond to multiple elements of the cohomology if there is a multiple of 3 S_1 sites per row, that is if $\vec{u} = (3n, -3n)$. This is a direct consequence of Theorem 5.1, which says that a periodic chain with length $3j$ has two ground states. In fact, these configurations account for 2^p elements each, where $p = (v_1 + v_2)/3$ is the total number of S_1 rows or, equivalently, of S_2 chains. On the other hand, for $\vec{u} = (m, -m)$ with $m \neq 3n$ they each represent one element of the cohomology. So we find $N^{(a)} = 2^{p+1}$ for $m = 3n$ and $N^{(a)} = 2$ otherwise.

Now, let us look at the corresponding tilings. For $\vec{u} = (m, -m)$ with $m \neq 3n$ there is no corresponding tiling, thus there is a discrepancy of 2 between the number of tilings and the number of elements in the cohomology. That is $\Delta \equiv N^{(a)} - t^{(a)} = 2$ for $m \neq 3n$. For $\vec{u} = (3n, -3n)$ there are tilings corresponding to the configurations with all zeroes or all dots. Along the $\vec{u}$ direction these tilings have periodicity 3. The periodicity in the other direction is more involved. Given the boundary condition $\vec{v} = (2r + s, r + 2s)$ the tiling makes r steps in the (2,1) direction and s steps in the (1,2) direction, in arbitrary order. However, because of the periodicity of 3 in

the $\vec{u}$ direction one can also end at $(2r+s+3l, r+2s-3l)$, that is, $r+3l$ steps in the (2,1) direction and $s-3l$ steps in the (1,2) direction, again in arbitrary order. Thus we find

$$t^{(a)} = 2 * 3 \sum_{l \geq -r/3} \binom{r+s}{r+3l}.$$

If we define $r = 3k + c$, where $c \in 0, 1, 2$, we can write t as:

$$\begin{aligned}
t^{(a)} &= 6 \sum_{l=0} \binom{r+s}{c+3l} \\
&= 6 \sum_{l=0} \left[\binom{r+s-2}{c+3l-2} + 2\binom{r+s-2}{c+3l-1} + \binom{r+s-2}{c+3l} \right] \\
&= 6 \sum_{l=0} \left[\binom{r+s-2}{l} + \binom{r+s-2}{c+3l-1} \right] \\
&= 6 * 2^{r+s-2} + 6 \sum_{l=0} \left[\binom{r+s-2}{c+3l-1} \right].
\end{aligned}$$

Repeating these steps d times, such that $2d \leq r+s$, we find

$$\begin{aligned}
t^{(a)} &= 6 \sum_{l=1}^{d} 2^{r+s-2l} + 6 \sum_{l=0} \binom{r+s-2d}{c+3l-d} \\
&= \sum_{l=0}^{2d-1} 2^{r+s-l} + 6 \sum_{l=0} \binom{r+s-2d}{c+3l-d} \\
&= \begin{cases} 2^{r+s+1} - 2 + 6 \sum_{l=0} \binom{0}{c+3l-d} & \text{if } r+s = 2d, \\ 2^{r+s+1} - 4 + 6 \sum_{l=0} \binom{1}{c+3l-d} & \text{if } r+s = 2d+1. \end{cases}
\end{aligned}$$

For the last term we find

$$6 \sum_{l=0} \binom{0}{c+3l-d} = \begin{cases} 6 & \text{if } d = 3b + c, \\ 0 & \text{otherwise.} \end{cases}$$

$$6 \sum_{l=0} \binom{1}{c+3l-d} = \begin{cases} 0 & \text{if } d = 3b + c + 1, \\ 6 & \text{otherwise.} \end{cases}$$

We now compare the expression for $t^{(a)}$ with the expression for the number of elements in the cohomology represented by the configurations with all zeroes and all dots, $N^{(a)}$. For $\vec{v} = (2r+s, r+2s)$ this is $N^{(a)} = 2 * 2^{(v_1+v_2)/3} = 2^{r+s+1}$. So we finally find

$$\Delta = N^{(a)} - t^{(a)} = \begin{cases} -4 & \text{if } r+s = 2d \text{ and } r-s = 6b, \\ 2 & \text{if } r+s = 2d \text{ and } r-s = 6b \pm 2, \\ 4 & \text{if } r+s = 2d+1 \text{ and } r-s = 6b+3, \\ -2 & \text{if } r+s = 2d+1 \text{ and } r-s = 6b \pm 1. \end{cases}$$

Combining this with the result $\Delta = 2$ for $\vec{u} = (m, -m)$ with $m \neq 3n$, this can be cast in the compact form of equation (4.2).

Acknowledgments

We would like to thank P. Fendley for discussions and J. Jonsson for suggested improvements of the manuscript.

References

[1] P. Fendley, K. Schoutens and J. de Boer, *Lattice models with $N = 2$ supersymmetry*, Phys. Rev. Lett. **90** (2003), 120402.

[2] P. Fendley, B. Nienhuis and K. Schoutens, *Lattice fermion models with supersymmetry*, J. Phys. **A36** (2003), 12399.

[3] M. Beccaria and G. F. De Angelis, *Exact ground state and finite size scaling in a supersymmetric lattice model*, Phys. Rev. Lett. **94** (2005), 100401.

[4] P. Fendley and K. Schoutens, *Exact results for strongly-correlated fermions in $2+1$ dimensions*, Phys. Rev. Lett. **95** (2005), 046403.

[5] H. van Eerten, *Extensive ground state entropy in supersymmetric lattice models*, J. Math. Phys. **46** (2005), 123302.

[6] L. Huijse and K. Schoutens, *Superfrustration of charge degrees of freedom*, Eur. Phys. J. **B64** (2008), 543–550.

[7] L. Huijse, J. Halverson, P. Fendley and K. Schoutens, *Charge frustration and quantum criticality for strongly correlated fermions*, Phys. Rev. Lett. **101** (2008), 146406.

[8] J. Jonsson, *Hard squares with negative activity and Rhombus Tilings of the plane*, Electron. J. Combin. **13**(1) (2006), #R67.

[9] J. Jonsson, *Certain homology cycles of the independence complex of grid graphs*, Discrete Comput. Geom. **43**(4) (2010), 927–950.

[10] J. Jonsson, *Hard squares on grids with diagonal boundary conditions*, preprint, 2006.

[11] R. J. Baxter, *Hard squares for $z = -1$*, preprint, 2007.

[12] M. Bousquet-Melou, S. Linusson and E. Nevo, *On the independence complex of square grids*, J. Algebraic Combin. **27** (2008), 423–450.

[13] A. Engström, *Upper bounds on the Witten index for supersymmetric lattice models by discrete Morse theory*, Eur. J. Combin. **30**(2) (2009), 429–438.

[14] P. Csorba, *Subdivision yields Alexander duality on independence complexes*, Electron. J. Combin. **16**(2) (2009), #R11.

[15] P. Fendley, K. Schoutens and H. van Eerten, *Hard squares at negative activity*, J. Phys. **A38** (2005), 315.

[16] R. Bott and L. W. Tu, *Differential forms in algebraic topology*, GTM, **82**, Springer Verlag, New York, 1982.

[17] E. Witten, *Constraints on supersymmetry breaking*, Nucl. Phys. **B202** (1982), 253.

[18] R. J. Baxter, *Hard hexagons: exact solution*, J. Phys. A: Math. Gen. **13** (1980), L61–L70.